Alternative Plating Processes for Metal Electroplating Based on Ionic Liquids

Project No: WP-2316

Performed by

Oak Ridge National Laboratory
University of Mississippi

Lead PI: Sheng Dai

Co-PIs: Xiao-Guang Sun
Chuck L Hussey

April 24, 2017

REPORT DOCUMENTATION PAGE

Form Approved
OMB No. 0704-0188

The public reporting burden for this collection of information is estimated to average 1 hour per response, including the time for reviewing instructions, searching existing data sources, gathering and maintaining the data needed, and completing and reviewing the collection of information. Send comments regarding this burden estimate or any other aspect of this collection of information, including suggestions for reducing the burden, to the Department of Defense, Executive Services and Communications Directorate (0704-0188). Respondents should be aware that notwithstanding any other provision of law, no person shall be subject to any penalty for failing to comply with a collection of information if it does not display a currently valid OMB control number.

PLEASE DO NOT RETURN YOUR FORM TO THE ABOVE ORGANIZATION.

1. REPORT DATE *(DD-MM-YYYY)*	2. REPORT TYPE	3. DATES COVERED *(From - To)*
April 24, 2017	SERDP Final Report	April 2017- Feb 2018

4. TITLE AND SUBTITLE

Alternative Plating Processes for Metal Electroplating Based on Ionic Liquids

Project No: WP-2316

5a. CONTRACT NUMBER
WP-2316

5b. GRANT NUMBER

5c. PROGRAM ELEMENT NUMBER

6. AUTHOR(S)
Xiao-Guang Sun, Sheng Dai, Chuck Hussey

5d. PROJECT NUMBER
WP-2316

5e. TASK NUMBER

5f. WORK UNIT NUMBER

7. PERFORMING ORGANIZATION NAME(S) AND ADDRESS(ES)

Oak Ridge National Laboratory
One Bethel Valley Road
Oak Ridge, TN 37831-6054

8. PERFORMING ORGANIZATION REPORT NUMBER
WP-2316

9. SPONSORING/MONITORING AGENCY NAME(S) AND ADDRESS(ES)

Strategic Environmental
Development Program (SERDP)
4800 Mark Center Drive
Alexandria, VA 22350-3605

10. SPONSOR/MONITOR'S ACRONYM(S)
SERDP

11. SPONSOR/MONITOR'S REPORT NUMBER(S) WP-2316

12. DISTRIBUTION/AVAILABILITY STATEMENT

Approved for public release; distribution is unlimited.

13. SUPPLEMENTARY NOTES

PUB ID 107170 - Performing Organization includes University of Mississippi

14. ABSTRACT

The objective of this proposal is to develop air and water stable ionic liquids and deepeutectic solvents (DES) for electrodeposition of aluminum that could address the Department of Defense (DoD) life-cycle cost and environmental issues related to weapon systems. In this project, several approacheshave been used to develop air- and water-stable ionic liquids and DESs for electrodeposition of aluminum.

15. SUBJECT TERMS

Alternative Plating Processes, Metal Electroplating, Ionic Liquids

16. SECURITY CLASSIFICATION OF:			17. LIMITATION OF ABSTRACT	18. NUMBER OF PAGES	19a. NAME OF RESPONSIBLE PERSON
a. REPORT	b. ABSTRACT	c. THIS PAGE			Leesa Laymance, ORNL TIO *Leesa Laymance*
U	U	U	UU	53	19b. TELEPHONE NUMBER *(Include area code)* 865-574-0182

Contents

Fig. 16. FT-IR spectrum of DPS and DPS/$AlCl_3$ (1:1).

Fig. 17. Cyclic voltammogram of DPS:$AlCl_3$ at different molar ratios on a platinum working electrode with aluminum wire as both counter and reference electrode. Start potential: 1.0 V. Scan rate: 100 mV/s.

Fig. 18. Digital image (A) and scanning electron micrograph (B) and Energy-dispersive X-ray spectroscopy analysis (C) of electrodeposited aluminum on copper substrates.

Fig. 19 Cyclic voltammograms of ionic liquid of (a) tetrahydrothiophene/$AlCl_3$ =1/1.2) at 65°C, (b) thioacetamide/$AlCl_3$ =1/1.2), (c) thiourea/$AlCl_3$ = 1/1.2 at room temperature. Scan rate: 100 mV/s.

Fig.20. Cyclic voltammogram of P888O:$AlCl_3$ at different molar ratio on a platinum working electrode with aluminum wire as both counter and reference electrode. Scan rate: 100 mV/s.

Fig.21. SEM image of aluminum deposition in $P_{888}O/AlCl_3$ (1:1.4) ionic liquid at 60 C for 5 h under a potential of a) -0.3 V; b) -0.5 V.

Fig. 22. Energy-dispersive X-ray spectroscopy analysis of Al deposition on Cu foil.

Fig. 23. Cyclic voltammograms of (a) EMImCl-$AlCl_3$ (1-1.5, in molar ratio) and those of the mixture of equal volume of EMImCl-$AlCl_3$ (1-1.5) with (b) Acetone, (c) Acetonitrile, (d) Tetrahydrofuran, (e) Toluene, and (f) dichloromethane on a Pt electrode (2 mm in diameter) under a scan rate of 100 mV/s at room temperature (Al wire was used as the counter and reference electrode).

Fig. 24. ^{27}Al NMR spectra of ionic liquid EMImCl-$AlCl_3$ (1-1.5, in molar ratio) and its mixtures with equal volume of different organic solvents

Fig. 25. FTIR spectra of acrylamide, acrylamide-$AlCl_3$(1-1, in molar ratio), poly(acrylamide-$AlCl_3$, 1-1 in molar ratio), EMImCl-$AlCl_3$ (1-1.5, in molar ratio) and polymer gel electrolyte based on poly(acrylamide-$AlCl_3$, 1-1 in molar ratio) containing 80wt% EMImCl-$AlCl_3$ (1-1.5, in molar ratio).

Fig. 26. Pictures of the membrane containing 60 wt% of (a) $AlCl_3$-EMIm.Cl.

Fig. 27. Temperature dependence of ionic conductivities of the gel polymer electrolytes based on polyacrylamide containing different amount of EMImCl-$AlCl_3$ (1-1.5, in molar ratio)

Fig. 28. Cyclic voltamograms of the electrolyte containing 60 wt% of EMImCl-$AlCl_3$ (1-1.5, in molar ratio) at 50 ^oC at a scan rate of 100 mV/s. Cu and Al plates were used as working and counter electrode, respectively.

Fig. 29. Cyclic voltamograms of the membrane containing 60 wt% of a) $AlCl_3$-4-propylpyridine (1.4:1) and b) $AlCl_3$-acetamide (1.2:1) at 40 ^oC. Scan rate: 100 mV/s. Cu and Al plates were used as working and counter electrode, respectively.

List of Acronyms

AIBN: azobisisobutyronitrile
$Al(Tf_2N)_3$: aluminum bis(trifluoromethanesulfonyl)imide
$AlTf_3$: aluminum triflate
AN: acetonitrile
BCP: bipolar current pulse polarization
BMIm.Tf: 1-butyl-3-methylimidazolium trifluoromethanesulfonate
$BMP.Tf_2N$: 1-butyl-1-methylpyrrolidinium bis(trifluoromethanesulfonyl)imide
CV: cyclic voltammetry
DCM: dichloromethane
DES: deep eutectic solvents
DBP: dibutylphathalate
EDX: energy-dispersive X-ray spectroscopy
EMIm.Cl: ethylmethylimidazolium chloride
$EMIm.Tf_2N$: 1-ethyl-3-methylimidazolium bis(trifluoromethanesulfonyl)imide
FCC: failed coating circuit
IL: ionic liquid
MCP: monopolar current pulse polarization
$MPPy.Tf_2N$: 1-propyl-1-methylpyrrolidinium bis(trifluoromethanesulfonyl)imide
MS: mass spectroscopy
N-BPCl: N-butylpyridinium chloride
NMR: Nuclear magnetic resonance
4-Pr-Py: 4-propyl-pyridine
PC: propylene carbonate
PDP: potential dynamic polarization
PVdF-HFP: Poly(vinylidene fluoride-co-hexafluoropropylene)
Rp: polarization resistance

Abstract

The objective of this proposal is to develop air and water stable ionic liquids and deep eutectic solvents (DES) for electrodeposition of aluminum that could address the Department of Defense (DoD) life-cycle cost and environmental issues related to weapon systems. In this project, several approaches have been used to develop air- and water-stable ionic liquids and DESs for electrodeposition of aluminum. The first approach is to synthesize stable aluminum salts to replace hygroscopic $AlCl_3$ that could be used to prepare ionic liquids for electrodeposition of aluminum. Large ligands, such as O and N-containing ligands, are used to replace small Cl atom, which could be less moisture sensitive because of their bulkiness. The second approach is to develop new aluminum cation based ionic liquids using different neutral ligands, such as N, S, and P-containing ligands, which could not only reduce moisture sensitivity of the ionic liquids but also generate more electroactive Al-containing cationic species to improve the efficiency during electrodeposition of aluminum. The third approach is to develop a convenient wrap-plating technique using polymer gel membranes. The polymer gel electrolyte membranes could cover the substrates to be plated like blankets, preventing interference of moisture and oxygen from the air during electrodeposition of aluminum. The fourth approach is to seal the ionic liquids inside a chamber to obtain a portable aluminum deposition system (PADs), not only reducing the moisture sensitivity of the ionic liquids but also increasing the flexibility of electrodeposition of aluminum. Parallel to the development of air and water stable ionic liquids for electrodeposition of aluminum, different parameters affecting aluminum deposition such as current density, co-solvent, current on/off duration of pulsed current plating method, anodization time, have also been systematically investigated in this project. The ionic liquids developed in this project can be used in the DOD's depots for electrodeposition of aluminum to address the corrosion problems. Particularly, PADS significantly increases the flexibility of electrodeposition of aluminum, which can be conveniently used for in-situ (on-field) reparation of the related parts of DOD weapon systems, saving both time and cost by eliminating back and forth shipments of the parts.

1. Objective

The objective of this proposal is to accelerate the application of ionic liquids and deep eutectic solvents (DES) in nonaqueous electroplating to address the Department of Defense (DoD) life-cycle cost and environmental issues related to weapon systems. We have explored the use of task-specific ionic liquids and deep eutectic solvents (DESs) that could mitigate the issues of air/water-stability associated with current electroplating baths for aluminum or aluminum alloys. In addition, new methods of enhancing the conformal coating while mitigating the environmental issues have also been explored. Furthermore, the stability of these nonaqueous plating baths under various operational environments have been investigated to determine the long-term viability of these plating technologies.

2. Technical Approach

To avoid using volatile and toxic organic solvents, chloroaluminate-based ionic liquids have been intensively investigated for use in electrodeposition of aluminum. These ionic liquids can be conveniently prepared by combining anhydrous $AlCl_3$ with an organic chloride such as 1-ethyl-3-methyl imidazolium chloride (EMIm.Cl) and N-butylpyridinium chloride (N-BPCl). Unfortunately, these ionic liquids can be only used in an inert-gas atmosphere because of the hygroscopic nature of $AlCl_3$ and the chloroaluminate. This has prevented practical application of these ionic liquids for electrodeposition of aluminum, especially for open filed military related applications.

To mitigate the above issues of $AlCl_3$ and chloroaluminate, several approaches have been used to develop air- and water-stable ionic liquids and DESs for electrodeposition of aluminum in this project. The first approach is to synthesize stable aluminum salts to replace hygroscopic $AlCl_3$ that could be used to prepare ionic liquids for electrodeposition of aluminum. Large ligands, such as O and N-containing ligands, are used to replace small Cl atom, which could be less moisture sensitive because of their bulkiness. The second approach is to develop new aluminum cation based ionic liquids using different neutral ligands to reduce the moisture sensitivity and improve the plating efficiency of the ionic liquids during electrodeposition of aluminum. This approach is similar to the first approach, i.e. partially replacing small Cl ligand with large neutral ligands. On the one hand, it could reduce moisture sensitivity of the ionic liquids; on the other hand, it could generate Al-containing cationic species, which are more active than anionic species of $Al_2Cl_7^-$ under electrodeposition condition. The third approach is to develop a convenient wrap-plating technique using polymer gel membranes to reduce the moisture sensitivity of the ionic liquids. The polymer gel electrolytes could function as blankets covering the substrates to be plated, not only providing electroactive ionic liquids for electrodeposition of aluminum but also preventing moisture and oxygen for the air to interfere electrodeposition of aluminum. The fourth approach is to seal the ionic liquids inside a chamber to obtain a portable aluminum deposition system (PADs), not only reducing the moisture sensitivity of the ionic liquids but also increasing the flexibility of aluminum electrodeposition. Parallel to the development of air and water stable ionic liquids for aluminum deposition, different parameters affecting aluminum deposition such as current density, co-solvent, current on/off duration of pulsed current plating method, anodization time, have also been systematically investigated in this project.

3. Result and Discussion

This section is roughly arranged per the approaches outlined in the technical section. In the first section, it discusses the development of new ionic liquids for electrodeposition of aluminum. The first task of development of new ionic liquids is to synthesize new aluminum salts to replace $AlCl_3$ because of the hygroscopic nature of the latter. Followed the discussion of new aluminum slats, it discusses the development of new ionic liquids *via* neutral ligands complexation to generate electroactive aluminum-containing cationic species. N, S, and P-containing ligands are used to synthesize new ionic liquids. In the second section, it discusses the development of polymer gel-based baths for electrodeposition of aluminum, considering the interactions between the functional groups of the polymer and the components of the ionic liquids. In the third section, it discusses electrodeposition of aluminum using ionic liquid bath. To optimize the influencing parameters, such as current density, co-solvent, current duration of pulsed current, anodization time etc., the eutectic mixture of 1-ethyl-3-methyl imidazolium chloride and $AlCl_3$ at a molar ratio of 1:1.5 is used. In the fourth section, it discusses electrodeposition of aluminum using portable aluminum deposition system (PADs). The effects of surface treatment of the substrate, deposition protocol (constant current *vs.* constant voltage) is discussed. Finally, the utilization of 12.5 V D battery to power the PADs for electrodeposition of aluminum is discussed.

3.1 Development of ionic liquids for electrodeposition of aluminum

3.1.1 Development of new aluminum salts for electrodeposition of aluminum

The main purpose of this subtask is to synthesize new aluminum salts to replace $AlCl_3$ for aluminum electrodeposition, which can reduce the moisture sensitivity of the ionic liquids. First, we have used aluminum triflate ($AlTf_3$) and aluminum bis(trifluoromethane sulfonyl)imide ($Al(Tf_2N)_3$) to prepare the electrolyte solutions. $Al(Tf_2N)_3$ was added to the ionic liquid of $EMIm.Tf_2N$ at a molar ratio of 1:10, whose CV shows no obvious aluminum stripping peak (**Fig. 1a**). $Al(Tf_2N)_3$ was also added to an alkylsulfone, which have been used to dissolve $AlCl_3$ to form the electrolyte supporting reversible aluminum deposition/stripping.[1, 2] **Fig. 1a** shows that with 0.5M $Al(Tf_2N)_3$ dissolved in methyl isopropyl sulfone, no aluminum deposition/stripping was observed either. $AlTf_3$ was used by Atushi Omote in a patent regarding rechargeable aluminum ion batteries that were assembled with $Al_2(MoO_4)_3$ as the cathode active materials, 50 mM $AlTf_3$ in butylmethylimidazolium trifluoromethanesulfonate (BMIm.Tf) as the electrolyte, and 100 μm aluminum foil as the anode.[3] It was claimed that the aluminum battery could be cycled for more than 100 cycles with a stable capacity of 123 mAh g^{-1}. For a battery exhibiting such a good cycling performance reversible aluminum deposition/stripping was required; unfortunately, no CV and charge/discharge profile were shown in the patent. To confirm this, we have synthesized $BMI.Tf_2N$ in which 50 mM $AlTf_3$ was dissolved. The CV in **Fig. 1b** clearly shows no aluminum deposition/stripping. Also, with 10 wt% propylene carbonate (PC) was added, no aluminum deposition/stripping was observed either. Furthermore, no aluminum deposition was obtained for the above two electrolyte solutions after holding the potential at -1.0V versus Al/Al^{3+} for 2hrs. Similar results were observed when BMIm.Tf was used instead of $BMIm.Tf_2N$.

Besides $AlTf_3$ and $Al(Tf_2N)_3$, we also synthesized new per-fluorinated aluminum salts and ionic liquids, as shown in **Fig. 2**. Hexafluoro-isopropanol was used to synthesize aluminum hexfluoro-isopropoxide and the corresponding ionic liquid, 1-butyl-3-methylimidazolium tetra(hexafluoro-isopropyl)aluminate. Hexafluoroisopropanol was reacted with triethylaluminum to get the desired aluminum hexafluoroisopropoxide. The ionic liquid, 1-butyl-3-methyl imidazolium tetra(hexafluoro-isopropyl)aluminate, was synthesized by reacting aluminum hexafluoroisopropoxide with lithium hexafluoroisopropoxide to get lithium tetra(hexafluoro-isopropyl)aluminate, which was then metathesized with 1-butyl-3-methylimidazolium chloride. Different ratios of aluminum hexafluoroisopropoxide and 1-butyl-3-methyl imidazolium tetra(hexafluoro-isopropyl)aluminate were mixed and cyclic voltammetry was characterized. As shown in **Fig 3** that both the pure ionic liquid, 1-butyl-3-methyl imidazolium tetra(hexafluoro-isopropyl)aluminate, and its mixture with aluminum hexafluoroisopropoxide show no reversible aluminum deposition/stripping. No aluminum deposition was observed after holding the potential at -1.0V for 2 hours.

We also synthesized an aluminum-containing ionic liquid (**Fig. 4**). In the first step, 4-propylpyridine was reacted with hydrochloric acid to obtain N-hydro-4-pyridinium chloride salt, which was then metathesized with lithium bis(trifluoromethanesulfonyl)imide to get the ionic liquid of N-hydro-4-pyridinium bis(trifluoromethanesulfonyl)imide, followed by reacting with triethylaluminum to obtain the ionic liquid of aluminum tris[(4-propylpyridinium bis(trifluoromethanesulfonyl) imide]. Similarly, we also synthesized the ionic liquid based on the same cation but tetrafluoroborate anion. Both ionic liquids are liquid at room temperature, unfortunately, only reduction peaks with no Al stripping peak were observed, indicating that two new Al based ionic liquids cannot be used for Al electrodeposition of aluminum.

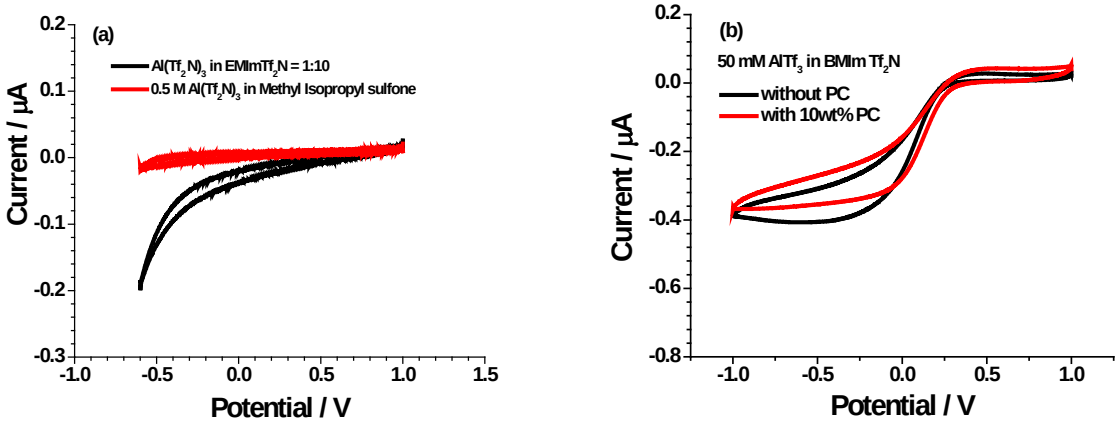

Fig.1. Cyclic voltammetry of (a) $Al(Tf_2N)_3$ in EMIM Tf_2N and methyl isopropyl sulfone and (b) $AlTf_3$ in BMIm Tf_2N with and without propylene carbonate (PC).

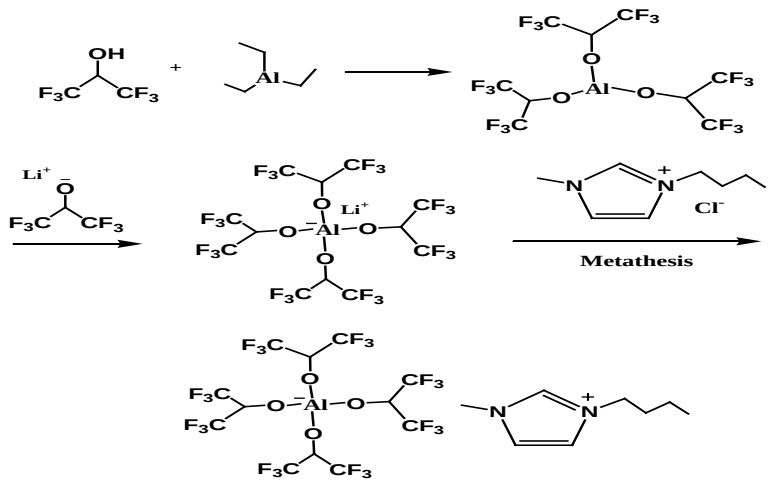

Fig.2. Synthesis of 1-butyl-3-methylimidazolium tetra(hexafluoro-isopropyl)aluminate

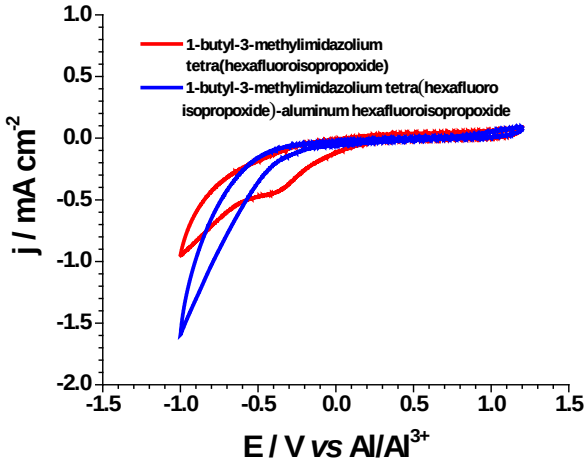

Fig. 3. Cyclic voltammograms of 1-butyl-3-methylimidazolium tetra(hexafluoroisopropoxide) with and without aluminum hexafluoroisopropoxide at a platinum electrode. Scan rate: 100 mV/s.

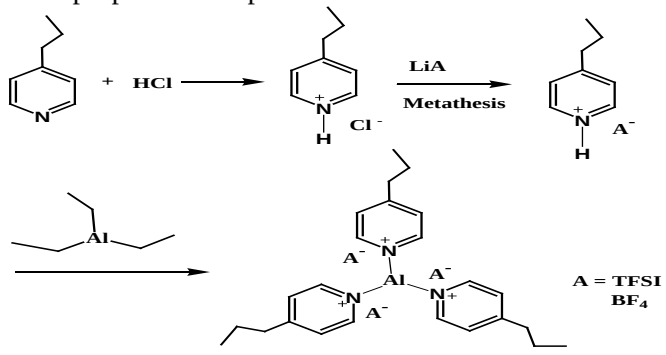

Fig.4. Synthesis of aluminum tris[(4-propylpyridinium bis(trifluoromethanesulfonyl) imide] and aluminum tris[(4-propylpyridinium tetrafluoroborate]

3.1.2 Development of new Ionic liquids based on neutral ligands

Most research on the use of ILs for electrodeposition of aluminum is still focused on chloroaluminate systems, first reported by Hurley and Wier in 1948.[4, 5] Later, Wilkes et al. reported aluminum deposition using the chloroaluminate IL based on 1-methyl-3-ethylimidazolium chloride (EMIm.Cl) and $AlCl_3$.[6] Since then, $AlCl_3$-imidazolium ILs have been widely used for electrodeposition of aluminum and its alloys, due to their desirable low melting points, high conductivity, and wide electrochemical windows.[7-12] A common feature of these chloroaluminate ILs for aluminum electrodeposition is that the electroactive species are aluminum-containing anionic species such as $Al_2Cl_7^-$. The disadvantage of anionic species for deposition is that under reductive conditions, they not only travel against the electric field but also compete with common cations such as N-alkyl pyridinium and imidazolium along the electric field, which will induce polarization and reduce the energy efficiency of the electrodeposition process. Therefore, development of ILs with aluminum-containing cations as the electroactive species is highly desirable.

Although ILs with Al-containing anions are very common, their counter parts with Al-containing cations are seldom reported. The formation of cationic aluminum complex species generally involves either the asymmetric cleavage of a halide-bridged dimeric compound or halide displacement, abstraction or elimination, in which a neutral ligand donor (or base) complexes with the cation to compensate the charge.[13] Following a similar approach, Abbott et al. recently reported that simple neutral amides such as acetamide and urea could be mixed with $AlCl_3$ to form room-temperature ILs, which were used both as catalysts for acetylation of ferrocene and as electrolytes for electrodeposition of aluminum.[14] Owing to the high concentration of functional groups ($–CONH_2$ or NH_2CONH_2) and short alkyl chains ($–CH_3$), these ILs cannot effectively shield the aluminum center and thus are still moisture-sensitive. In this section, we have used different neutral ligands, including N-containing neutral ligands, S-containing neutral ligands, and P-containing neutral ligands, to synthesize ionic liquids for electrodeposition of aluminum.

3.1.2.1 Ionic liquids based on $AlCl_3$ and N-containing neutral ligands

We have synthesized a new IL based on $AlCl_3$ and a derivative of pyridine, 4-propylpyridine (4-Pr-Py). This new IL based on complexation with neutral ligands is fundamentally different from earlier ones based on the mixing of $AlCl_3$ and N-alkyl pyridinium halide salts. First, the positive charge is on the aluminum in the former case, whereas it is localized on the pyridium cation in the latter case. Second, under reductive conditions, the neutral pyridine species are more stable than the cationic pyridinium species; therefore, they will not be reduced during the aluminum deposition process and affect the morphology. Finally, as mentioned earlier, the cationic aluminum species are more favored than anionic aluminum species for electrodeposition of aluminum.

The new IL was prepared by slowly adding calculated amounts of $AlCl_3$ into 4-Pr-Py under magnetic stirring in an Ar-filled glove box. $AlCl_3$ quickly reacts with 4-Pr-Py with heat being released. The cooled solution remains liquid at room temperature as long as the mixing molar ratio of $AlCl_3$ and 4-Pr-Py is in the range of 1.1:1 to 1.5:1. The formation of ILs (or complexes) between $AlCl_3$ and 4-Pr-Py can be verified by thermal gravimetric analysis (TGA). As shown in

Fig. 5, under an inert atmosphere of helium and a heating rate of 20°C/min, 4-Pr-Py starts evaporating slowly at the very beginning with a major onset temperature of 95°C. For $AlCl_3$, the major evaporation onset temperature is 160°C. When the mixing ratio of $AlCl_3$ and 4-Pr-Py is 1:1, the onset temperature is increased to 270°C. Increasing the ratio of $AlCl_3$ and 4-Pr-Py to 1.3:1, the onset temperature drops to 250°C. Nonetheless, the onset decomposition temperatures of the complexes are significantly higher than those of each of the components, confirming that complexes are formed.

Mass spectra (MS) measurement was also used to observe the molecular and quasi-molecular ion peaks. A typical example of the MS spectra for $AlCl_3$/4-Pr-Py (1.1:1) is shown in **Fig. 6**. Mass-to-charge ratios of m/z = 121 and 340 in the positive spectrum (Fig. 4a), can be assigned to [4-Pr-Py] and $[AlCl_2(4\text{-Pr-Py})_2]$, respectively. Similarly, a value of m/z = 169 in the negative mass spectrum (Fig. 4b) is attributed to $[AlCl_4]^-$. However, $Al_2Cl_7^-$ (m/z = 275.5) is not observed in the spectra, similar to the previously reported IL based on complexation of amide and $AlCl_3$.[14] It is assumed that the disproportionation of $AlCl_3$ generates $AlCl_2^+$ and $AlCl_4^-$, and the former is coordinated by 4-Pr-Py. The general formation can be summarized as follows:

$$2AlCl_3 + 2\ 4\text{-Pr-Py} \leftrightarrow [AlCl_2(4\text{-Pr-Py})_2]^+ + AlCl_4^- \quad (1)$$

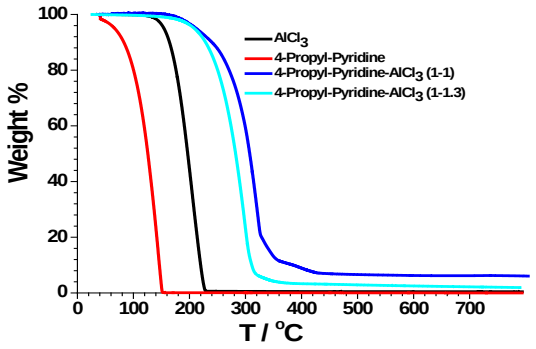

Fig. 5 Thermal gravimetric analysis diagrams of $AlCl_3$, 4-propylpyridine, and their complexes at different molar ratios under an inert atmosphere of helium with a heating rate of 20°C/min.

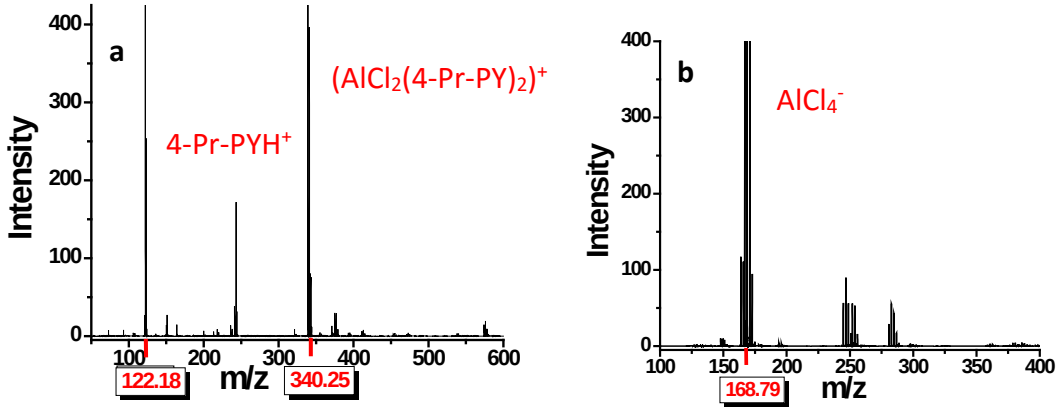

Fig. 6. MS spectrum of $AlCl_3$/4-Pr-Py (1.1:1) (left: positive ions; right: negative ions)

Nuclear magnetic resonance (NMR) was also used to identify the coordinated aluminum species in the new ILs, with the well-studied EMIC/$AlCl_3$ IL as a reference. As seen in **Fig. 7,** there is a peak only at 103 ppm for the EMIC/$AlCl_3$ IL with a molar ratio of 1:1, which can be attributed to the anion of $AlCl_4^-$/$Al_2Cl_7^-$. As a comparison, there are two peaks, at 103 ppm and 108 ppm, for the $AlCl_3$:4-Pr-Py IL with the same molar ratio of 1:1. Note that the broad peak around 69 ppm appeared on all IL sample results from the NMR tube. The peak at 103 ppm can also be attributed to the anion of $AlCl_4^-$, and the other one at 108 ppm can be assigned to the cation of $[AlCl_2(4\text{-Pr-Py})_2]^+$. The two coordinated aluminum species from the NMR spectra are consistent with those from MS results. However, with more $AlCl_3$ is added to the $AlCl_3$/4-Pr-Py IL, $AlCl_3$/4-Pr-Py=1.3:1, the peak at 108 ppm becomes broader and overlaps with the peak at 103 ppm.

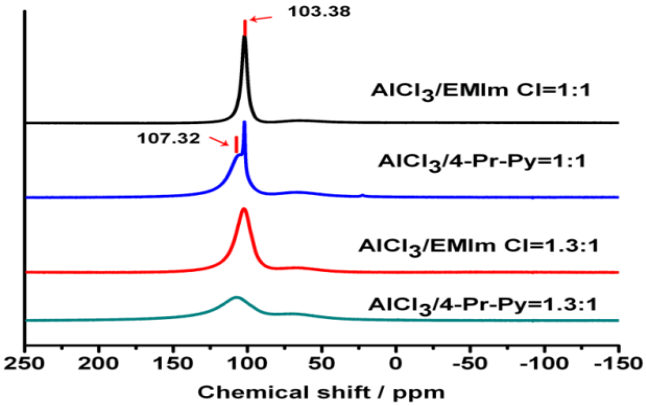

Fig. 7. ^{27}Al NMR spectra of $AlCl_3$/EMIm Cl ILs and $AlCl_3$/4-PrPy ILs in different molar ratio.

Ionic conductivities of the new ILs were measured using electrochemical impedance spectra with a self-made two-platinum-electrode cell calibrated with a 0.1M KCl aqueous solution. **Fig. 8** shows the temperature dependence of the ionic conductivities of the ILs. The ionic conductivity is the lowest when the molar ratio of $AlCl_3$ and 4-Pr-Py is 1:1. With more $AlCl_3$ being added, the ionic conductivity increases significantly. The highest ambient ionic conductivity of 5.0×10^{-4} S/cm is obtained for the IL with a molar ratio of $AlCl_3$ and 4-Pr-Py being 1.3:1, which will be used for the cyclic voltammetry (CV) measurement and electrodeposition of aluminum.

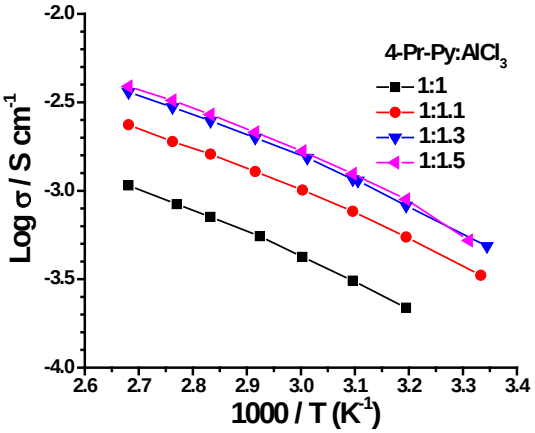

Fig. 8. Temperature dependence of ionic conductivities of of $AlCl_3$:4-Pr-Py at different molar ratios.

Fig. 9 shows the cyclic voltammogram of the IL on a platinum working electrode at a scan rate of 100 mV/s. The aluminum deposition starts at a potential of –0.16 V vs Al/Al^{3+}, and there is a corresponding aluminum stripping peak at 0.35 V. It was noticed that the bulk deposition region shows a characteristic "nucleation loop" where the forward and backward current cross over.[15] The bulk electrolysis was carried out using a polished copper strip as cathode, spiral aluminum wire as counter electrode, and straight aluminum wire as reference electrode. Based on the CV data in **Fig. 9**, the bulk electrolysis was carried out using a potentiostatic method; that is, a constant potential of –0.2 V *vs* Al/Al^{3+} was used. The electrolysis was carried out for 1 and 3 h, respectively. **Fig. 10a** shows the digital images (A and C) and scanning electron micrographs (B and D) of the electrodeposited aluminum on the copper substrates. A homogeneous, bright, adherent aluminum layer was obtained after plating for only 1 h (B in **Fig. 10a**). When the plating time was increased to 3 h, a thicker and uneven aluminum deposition was obtained (D in **Fig. 10a**). To confirm the purity of the deposition, the 1 h deposition film was further analyzed with x-ray diffraction and energy–dispersive x-ray spectroscopy. As shown in **Fig. 10b & c**, indeed there are only signals of the substrate copper and the deposited aluminum. Similarly, ionic liquids based on longer alkyl chain pyridines such as 2-butylpyridine was also prepared. It has lower melting point than that based on 4-propylpyridine and is much better candidate for aluminum deposition.

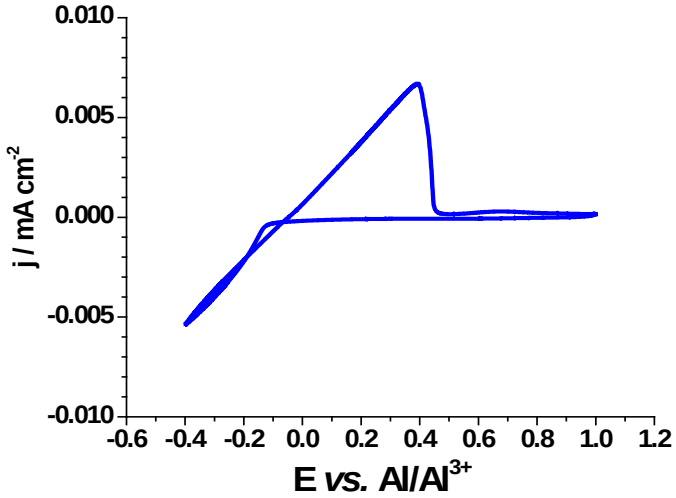

Fig. 9. Cyclic voltammogram of $AlCl_3$:4-Pr-Py at a molar ratio of 1.3:1 on a platinum working electrode with aluminum wire as both counter and reference electrode. Scan rate: 100 mV/s.

In addition to 4-propylpyridine, we also investigated cheaper N-containing ligands such as urea. Urea can form ionic liquids with $AlCl_3$ in the molar ratio range of 1 to 1~1.3. **Fig. 11a** shows the CV of the ionic liquid of urea/$AlCl_3$ = 1/1.3, exhibiting reversible aluminum deposition/stripping. The electrodeposited aluminum is grayish as shown in **Fig. 11b,** not as bright as the deposits from other ligands.

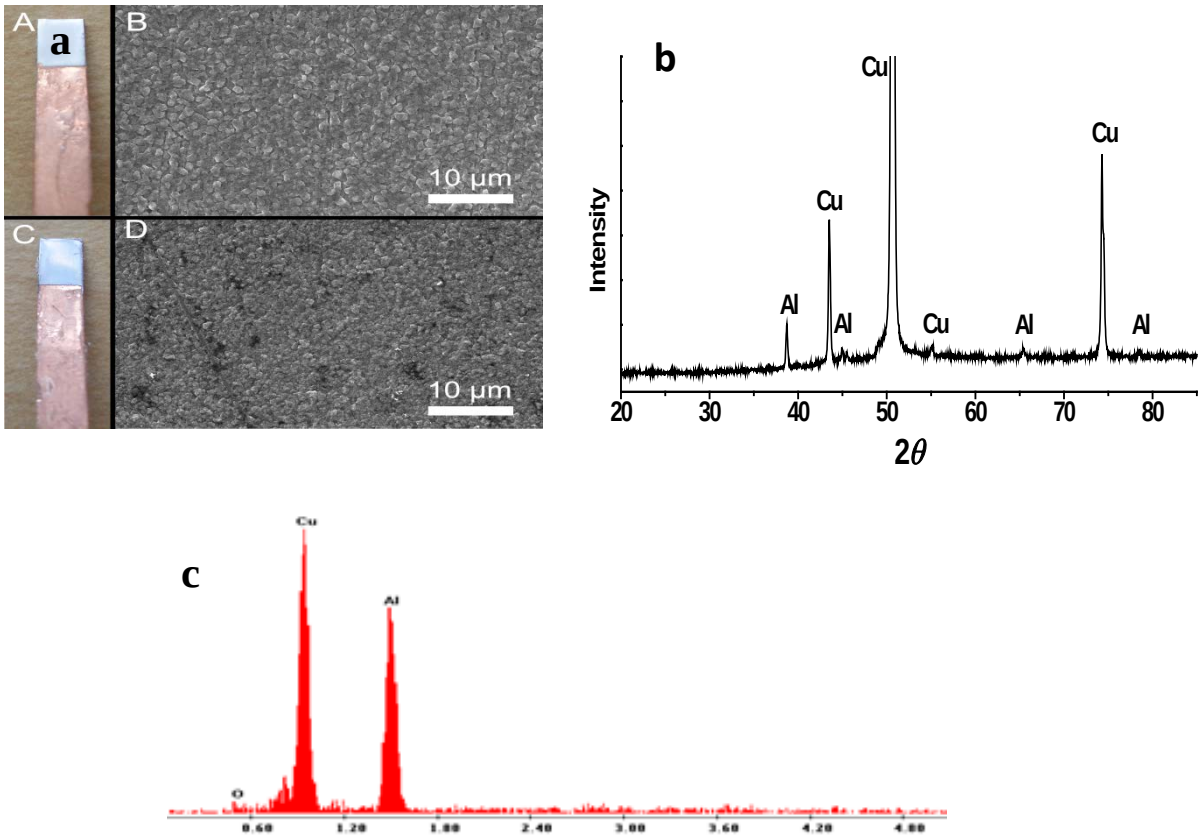

Fig. 10 (a). Scanning electron micrographs (A and C) and digital images of aluminum deposition on copper substrates (B and D). Electrodeposition was performed by the potentiostatic method (–0.2 V vs. Al/Al^{3+}) in the ionic liquid of $AlCl_3$ and 4-propylpyridine with a molar ratio 1.3:1 for 1 h (A and B) and 3 h (C and D) at room temperature; (b) X-ray diffraction pattern of Al deposition on Cu foil; (c) Energy-dispersive X-ray spectroscopy (EDX) analysis of Al deposition on Cu foil.

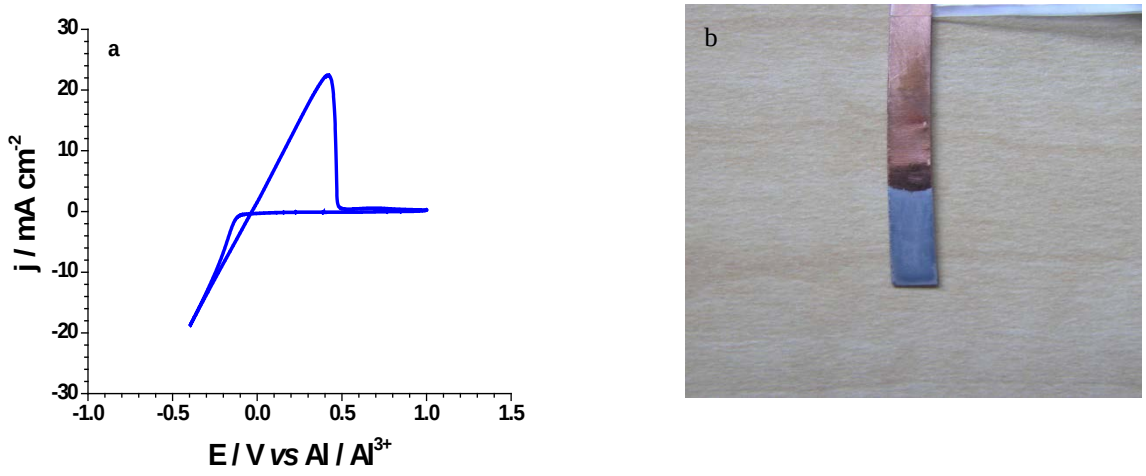

Fig. 11 (a) Cyclic voltammograms of ionic liquid of urea/$AlCl_3$=1/1.3 at room temperature. Scan rate: 100 mV/s; (b) Digital image of electrodeposited aluminum on Cu using ionic liquid of urea/$AlCl_3$=1/1.3.

3.1.2.2 Ionic liquids based on $AlCl_3$ and S-containing neutral ligands

In principle, group VI elements also possess lone pair electrons and they should be able to form ionic liquids with $AlCl_3$, like V elements, however, Al-RTILs based on ligands from group VI elements such as O and S have hardly been investigated. We tried to obtain ionic liquids using simple oxygen containing solvents such as tetrahydrofuran (THF), dimethoxyethane (DME), and tetraethylene glycol dimethyl ethers as the complexing ligands for $AlCl_3$. Unfortunately, even though these ethers can dissolve some $AlCl_3$ but hardly reach 1:1 molar ratio with $AlCl_3$. As a result, the CVs show no reversible aluminum deposition/stripping.

Fig. 12 Digital photo of DPS/$AlCl_3$ (1:1.05, molar ratio) IL.

We then focus on preparing new Al-RTILs based on $AlCl_3$ and S-containing ligands, whereas dipropyl sulfide (DPS) was used as an example. DPS can interacts with $AlCl_3$ to produce both Al-containing cation and anion by the asymmetric cleavage of $AlCl_3$, as confirmed by mass spectrometry (MS) and infrared spectroscopy. The DPS/$AlCl_3$ ILs were prepared by adding calculated amount of $AlCl_3$ into DPS with stirring in an Ar-filled glove box. External heat might be needed to get more $AlCl_3$ reacted A high molar ratio of 1:1.05 between DPS and $AlCl_3$ can be readily obtained, producing a near colorless (slightly yellow) liquid with a low viscosity of 6.87 mPa•s at room temperature (**Fig. 12**).

Direct analysis in real time mass spectrometry (DART-MS) was used to identify the cations and anions produced by the reaction between DPS and $AlCl_3$. As shown in **Fig. 13**, both cationic species $[AlCl_2(DPS)_2]^+$ and anionic species $AlCl_4^-$ are directly observed, however, $Al_2Cl_7^-$ is not found in the MS spectrum. This result is similar to those previously reported for the ILs based on the complexation of "neutral" ligands and $AlCl_3$. [9, 11] It is assumed that the asymmetric cleavage of $AlCl_3$ generates $AlCl_2^+$ and $AlCl_4^-$, with the former being coordinated with DPS, according to the following equation:

$$2AlCl_3 + 2\ DPS \leftrightarrow [AlCl_{2(}DPS)_2]^+ + AlCl_4^- \quad (2)$$

It should be noted that some intense peaks are difficult to identify, which might be due to the fragments produced during the ionization and recombination processes.

The ionic conductivities of DPS/$AlCl_3$ ILs were measured by electrochemical impedance spectroscopy with a self-made two-platinum-electrode cell calibrated with a 0.1 M KCl aqueous solution.[12] **Fig. 14** shows the temperature dependence of the ionic conductivities of the ILs.

Generally, the ionic conductivity can be described by the Arrhenius equation $\sigma = Ae^{-Ea(\sigma)/(RT)}$, where T is temperature, *A* is a coefficient, E_a is the activation energy and R is the universal gas constant. A calculated average E_a of the DPS/$AlCl_3$ ILs is 33.80 kJ/mol. It is interesting to note that the ionic conductivities can be obviously divided into two segments with 50 °C as a transition point. This might be related to the solid like transition around 40 °C observed in the DSC scan in **Fig. 15**. However, the source of the transition is unknown, which could be related to the impurity of DPS. For the ionic conductivity above 50 °C, a clear trend can be observed. For example, the ionic conductivity increases with increasing the molar ratio of $AlCl_3$ from 0.8 to 1.0, which can be attributed to the equilibrium of reaction (2) shifting to the right, that is, more ionic species are generated. However, the ionic conductivity decreases when the molar ratio of $AlCl_3$ is further increased to 1.05, which might be due to the increased viscosity of the ionic liquid. [11]

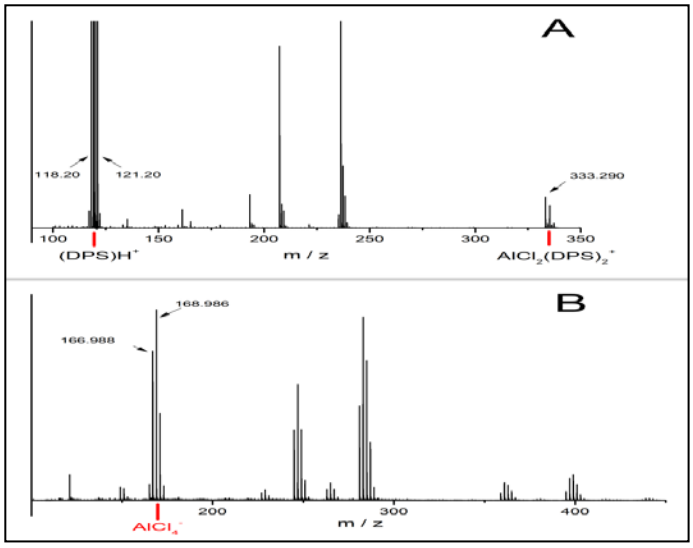

Fig. 13. MS spectrum of DPS/$AlCl_3$ (1:1.05) (DPS= dipropyl sulfide, A: cationic species; B: anionic species).

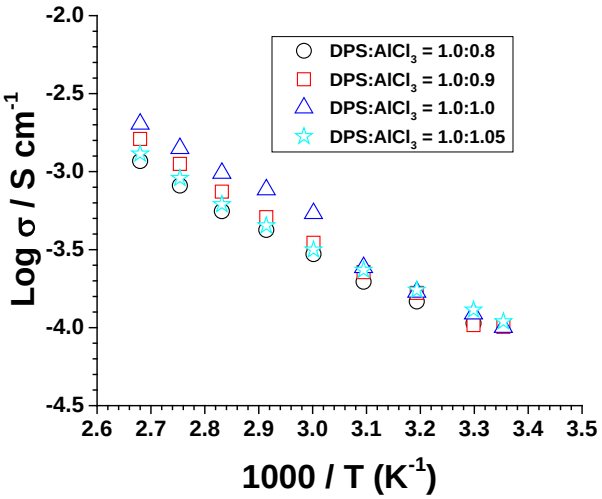

Fig. 14. Temperature (from 25 to 100 °C) dependence of ionic conductivities of ionic liquids on different molar ratios of DPS:$AlCl_3$.

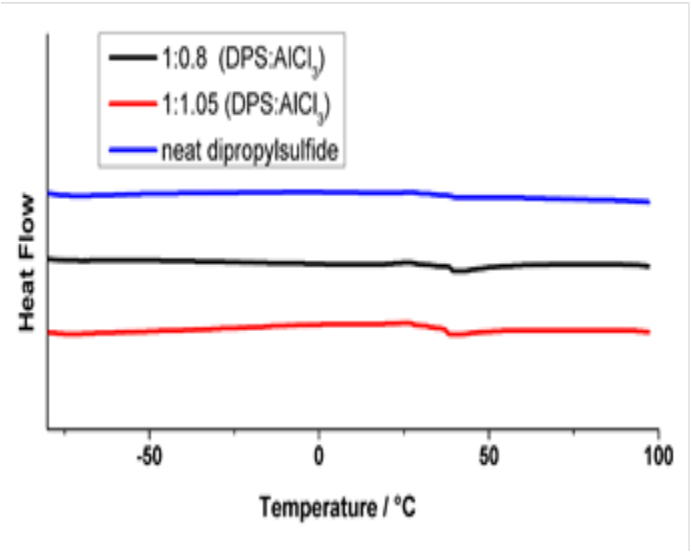

Fig. 15. DSC thermograms of the ionic liquids with different ratios of DPS/$AlCl_3$ at a heating rate of 10 °C /min under nitrogen. (Note: the lines have been shifted perpendicularly for clarity).

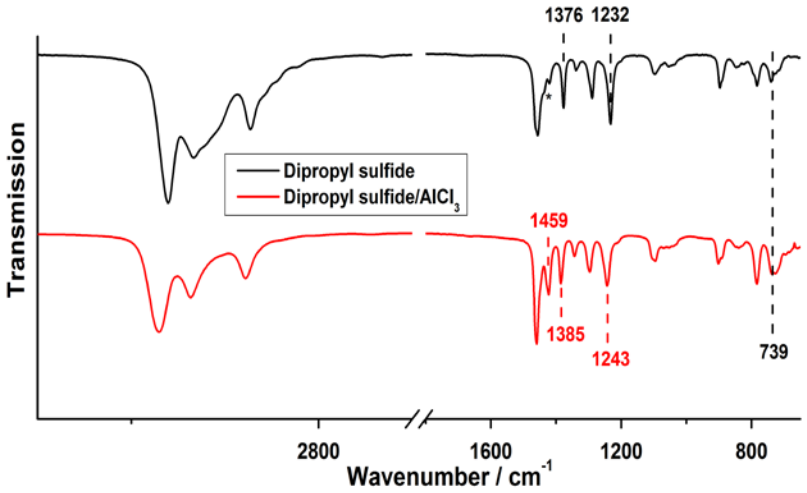

Fig. 16. FT-IR spectrum of DPS and DPS/$AlCl_3$ (1:1).

The reaction between DPS and $AlCl_3$ was also investigated by IR spectra in order to examine the effect of $AlCl_3$ complexation.[13] As shown in **Fig. 16**, the peak at 739 cm^{-1} can be attributed to C-S stretching vibration of DPS (black), which becomes broader after complexation with $AlCl_3$. The C-H wagging and twisting vibration peaks shift from 1232 and 1376 for neat DPS to 1243 and 1385 cm^{-1} after complexation with $AlCl_3$, respectively. Similar peak shifts were also observed for the complexation between pyridine and $AlCl_3$.[11] It was also observed that the characteristic peaks gradually shifted to higher wavenumbers with increasing the acidity of the IL.[14] The above observed IR spectra shifts further confirm that new IL is generated from the complexation of $AlCl_3$ and DPS *via* Al-S coordination interaction.

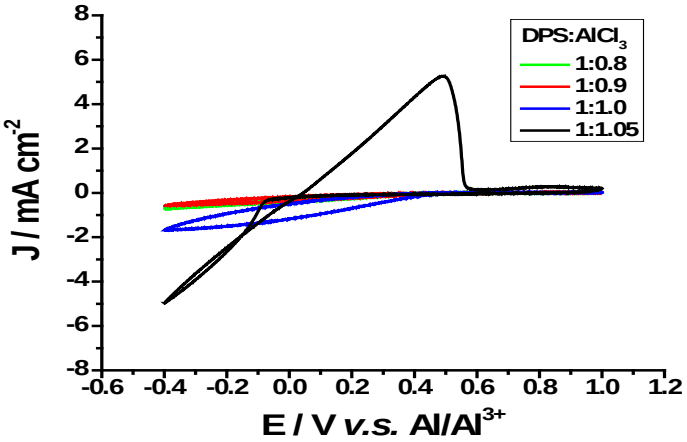

Fig. 17. Cyclic voltammogram of DPS:$AlCl_3$ at different molar ratios on a platinum working electrode with aluminum wire as both counter and reference electrode. Start potential: 1.0 V. Scan rate: 100 mV/s.

Fig. 17 shows the cyclic voltammograms of the ILs on a platinum working electrode under a scan rate of 100 mV/s at room temperature. Apparent aluminum deposition/stripping are observed for the IL with a molar ratio of 1:1.05 between DPS and $AlCl_3$ (black line). [4, 15] A characteristic "nucleation loop" is also noted for the above IL. [16] However, no reversible aluminum deposition/stripping can be observed for the ILs with lower $AlCl_3$ contents. It has been reported for the ILs based on quaternary ammonium halide salts and $AlCl_3$ that only the acidic ones support reversible Al deposition/stripping. [17, 18] However, for "neutral" ligands based ILs, this may be different for the following reasons: 1) Al deposition is possible for acetamide/$AlCl_3$ based IL with equal molar ratio of the two components;[9] 2) anionic species $Al_2Cl_7^-$ cannot be observed in the MS spectra for neutral ligand based ILs. [9, 11, 19] Unfortunately, the detailed reduction mechanism is still not clear, and we speculate that the Al-containing cations are the electroactive species. To check the possibility of electroplating Al using this IL, a constant current density of 4 mA/cm^2 was applied at 50 °C for 2 h with copper plate as the working electrode and Al as the counter electrode. **Fig. 18A** shows that the Cu substrate is covered by a white-gray deposit after the electrodeposition. A SEM image also shows fine grain-like Al crystals (**Fig. 18B**), which are similar to our previous results using pyridine based ILs.[11] EDS (Energy-dispersive X-ray spectroscopy) analysis is also used to identify the composition of the electrodeposited film. As shown in **Fig. 18C** that the deposition film is composed of pure Al without sulfur contamination. The ability to electrodeposit aluminum from this IL suggests the new sulfide/$AlCl_3$ IL indeed can be used for electrodeposition of aluminum.

In addition to use alkyl-sulfide as neutral ligand, tetrahydrothiophene, thioacetamide, and thiourea were also used to prepare the ionic liquid for electrodeposition of aluminum. All these ligands can form ionic liquids with $AlCl_3$. For instance, thiourea can form the ionic liquid with $AlCl_3$ in the molar ratio range of 1 to 1.0~1.2. Thioacetamide can form the ionic liquid with $AlCl_3$ in the molar ratio range of 1 to 0.9~1.1. Tetrahydrothiophene can form the ionic liquid with $AlCl_3$ in the molar ratio range of 1 to 0.9~1.2. The corresponding CVs of the three ionic liquids in **Fig. 19a, b & c** show reversible aluminum deposition/stripping. However, during electrodeposition black coatings were found on the surface of the copper substrate.

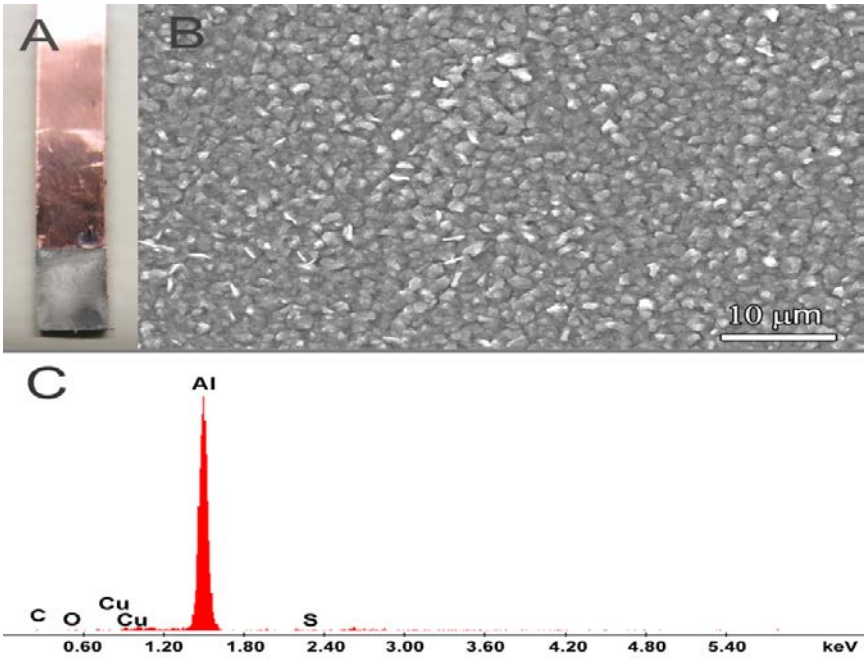

Fig. 18. Digital image (A) and scanning electron micrograph (B) and Energy-dispersive X-ray spectroscopy analysis (C) of electrodeposited aluminum on copper substrates.

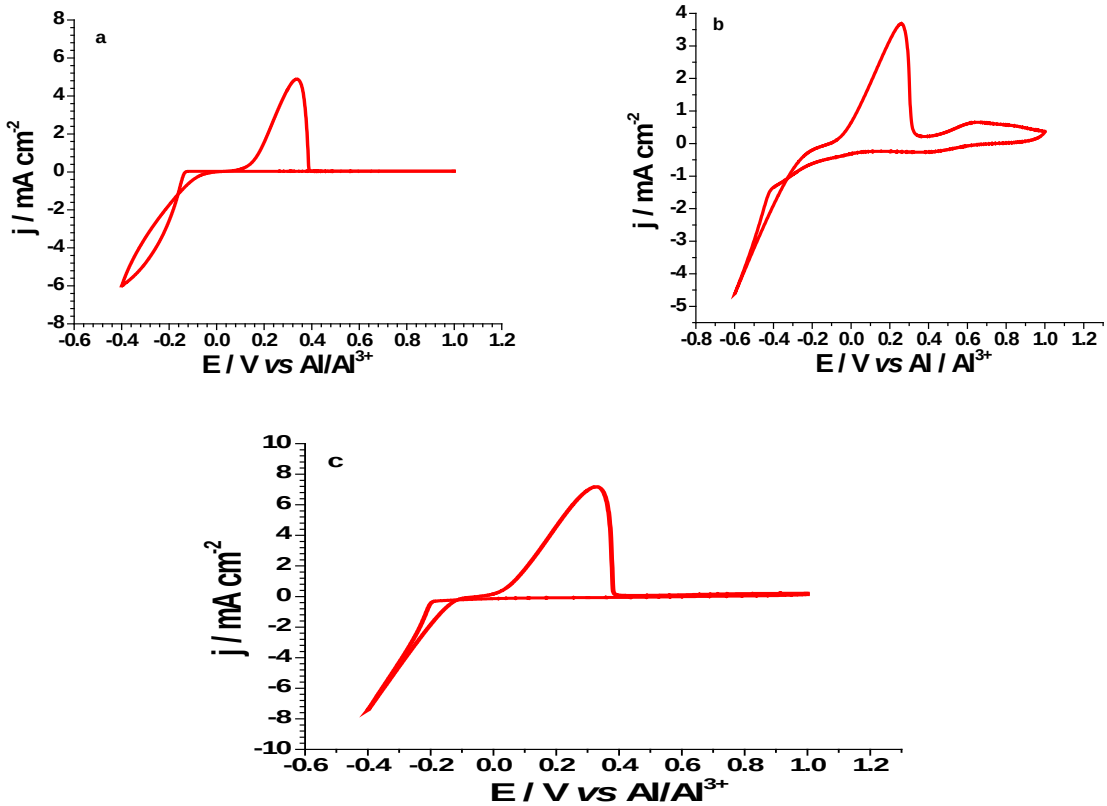

Fig. 19. Cyclic voltammograms of ionic liquid of (a) tetrahydrothiophene/$AlCl_3$ =1/1.2) at 65°C, (b) thioacetamide/$AlCl_3$ =1/1.2), (c) thiourea/$AlCl_3$ = 1/1.2 at room temperature. Scan rate: 100 mV/s.

3.1.2.3 Ionic liquids based on $AlCl_3$ and P-containing neutral ligands

After exploring the N and S-containing neutral ligands, we extend our effort to identify suitable P-containing neutral ligands to form ionic liquids with $AlCl_3$. Trialkylphosphines are pyrophoric, so we focused on trialkylphosphine oxides. It is noticed that Al reduction can only be observed when the molar ratio of $AlCl_3$ is greater than 1.2. In addition, during the preparation of the ILs heating can causes a "polymerization-like" process, making it difficult for Al electrodeposition. Furthermore, higher concentrations of $AlCl_3$ result in the solidification of the ionic liquids. **Fig. 20** shows CVs of the $P_{888}O/AlCl_3$ ionic liquids at different molar ratios at room temperature. As the concentration of $AlCl_3$ increases, the reduction current of Al increases, although not as dramatic as previously observed for the less viscous systems.

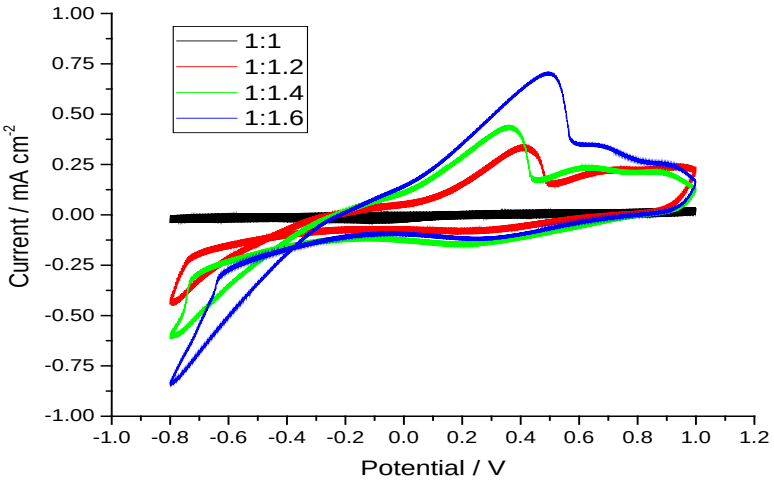

Fig.20. Cyclic voltammogram of P888O:$AlCl_3$ at different molar ratio on a platinum working electrode with aluminum wire as both counter and reference electrode. Scan rate: 100 mV/s.

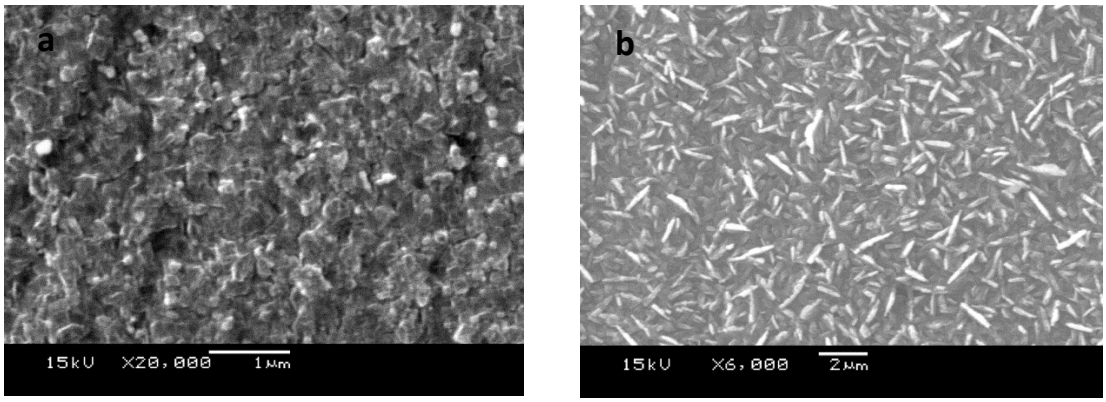

Fig.21. SEM image of aluminum deposition in $P_{888}O/AlCl_3$ (1:1.4) ionic liquid at 60 C for 5 h under a potential of a) -0.3 V; b) -0.5 V.

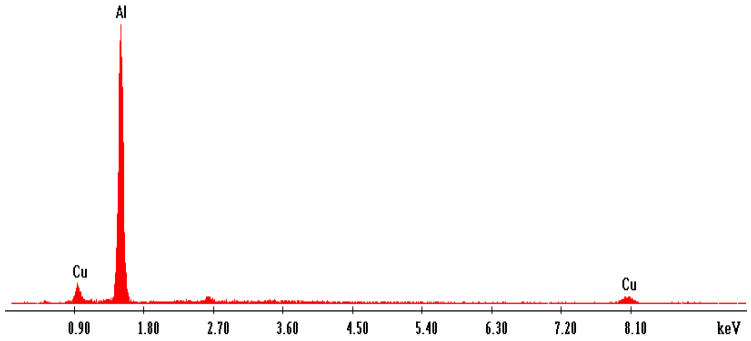

Fig. 22. Energy-dispersive X-ray spectroscopy analysis of Al deposition on Cu foil.

The electrochemical deposition was carried out at 60 ^{o}C using the ionic liquid of $P_{888}O/AlCl_3$ with a molar ratio of 1:1.4. Constant potentials of -0.5 V and -0.3 V were held for 5 hours during electrodeposition, respectively. As shown in the SEM images in **Fig. 21,** two kinds of Al morphologies are obtained. The grain-like Al is obtained by applying -0.3 V, whereas needle-like Al is obtained by applying -0.5 V. The different morphology might be due to the difference of the number of seedlings produced at different over potentials. The higher the over potential (-0.5V) produces more seedling than that at lower over potential (-0.3V), resulting in needle-like morphology in the former and grain-like morphology in the latter. As confirmed by EDS in **Fig. 22**, only Al is detected beside the Cu peaks (arise from Cu substrate). Thus, pure Al can be produced from $P_{888}O/AlCl_3$ ionic liquid without any contaminations.

3.2 Development of polymer gel-based baths for electrodeposition of aluminum

Even though chloroaluminate based ionic liquids with lower viscosities and higher ionic conductivities are good candidates for aluminum deposition, they are moisture sensitive due to the presence of $AlCl_3$. One of the effective ways to reduce the moisture sensitivity of these ionic liquids is to soak them in a polymer matrix, i.e. formation of polymer gel electrolytes, which can act as a protection shield for moisture. The polymer gel electrolytes are usually obtained by impregnating liquid electrolytes into the preformed electrolytes or co-cast polymer and liquid electrolytes, [16, 17] or by copolymerization of monomers in the presence of plasticizers. [18] The ultimate polymer gel electrolytes with reversible aluminum deposition/stripping not only can alleviate the moisture sensitivity issue of the chloroaluminate based ionic liquids for aluminum deposition but also can benefit the development of shape-flexible rechargeable aluminum ion batteries.

To obtain polymer gel electrolytes, suitable solvents have to be used in which both ionic liquids and monomers are soluble, but no reaction (or interaction) between the solvent and the gel electrolyte components is preferred. Thus, we have selected common solvents with low boiling points such as acetone, acetonitrile, tetrahydrofuran (THF), toluene and dichloromethane (DCM) as a diluent for the acidic eutectic mixture of EMImCl-$AlCl_3$ (1-1.5). Cyclic voltammetry (CV) is used as a screening technique for the selection of solvents. **Fig. 23** shows the CVs at a scan rate of 100 mV/s for EMImCl-$AlCl_3$ (1-1.5) and its mixtures with equal

volume of the aforementioned solvents. Without any diluent solvents, the CV of the pure ionic liquid, EMImCl-$AlCl_3$ (1-1.5), shows well defined Al deposition and stripping peaks, similar to that reported in the literature. [6] However, after mixing with organic solvents, the CVs show dramatic changes. As is well established in the literature that the reversible aluminum deposition/stripping in the acidic ionic liquid of EMImCl-$AlCl_3$ (1-1.5) is mainly due to the formation of electrochemically

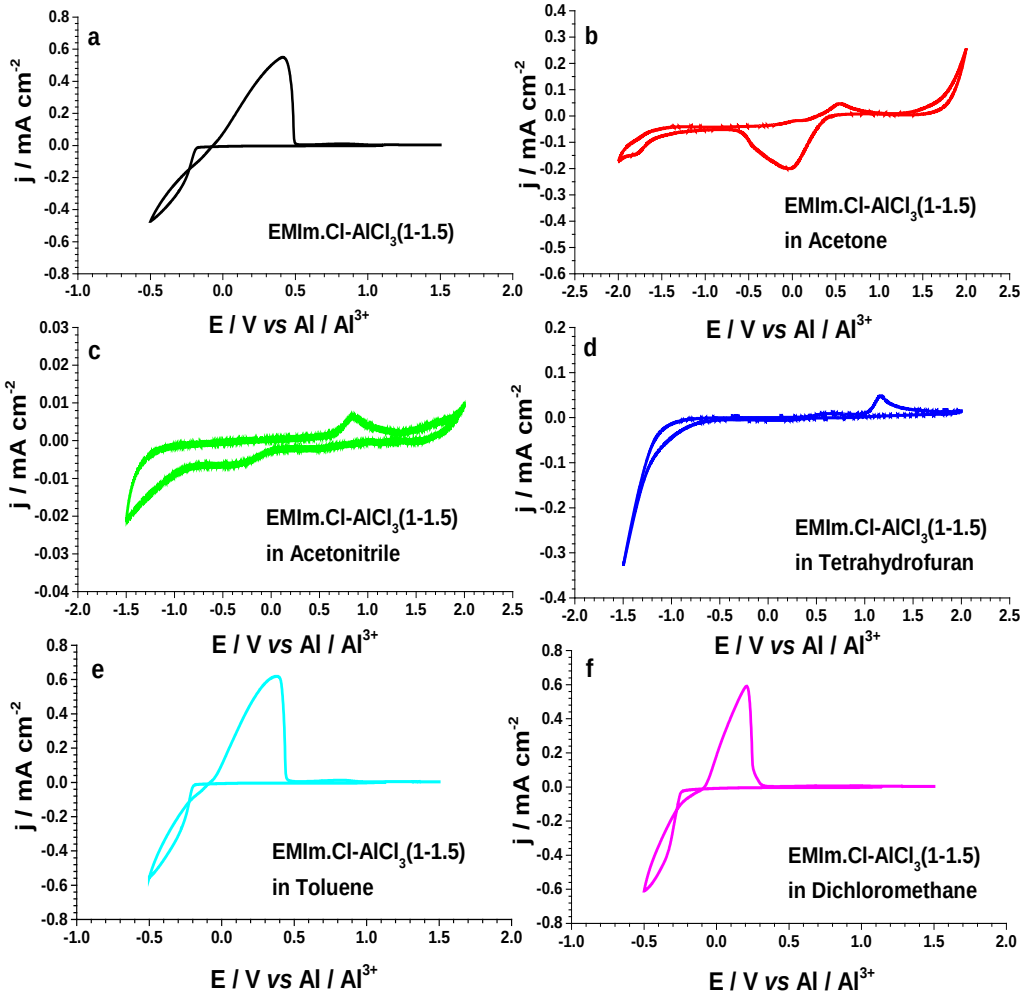

Fig. 23. Cyclic voltammograms of (a) EMImCl-$AlCl_3$ (1-1.5, in molar ratio) and those of the mixture of equal volume of EMImCl-$AlCl_3$ (1-1.5) with (b) Acetone, (c) Acetonitrile, (d) Tetrahydrofuran, (e) Toluene, and (f) dichloromethane on a Pt electrode (2 mm in diameter) under a scan rate of 100 mV/s at room temperature (Al wire was used as the counter and reference electrode).

active species of $Al_2Cl_7^-$ from the excess $AlCl_3$. [19] The electron-deficient $AlCl_3$ intends to interact or react with molecules bearing electron lone pairs. Indeed, when the ionic liquid is mixed such solvents like acetone, acetonitrile or THF, exothermal reaction happens. As a result, the interaction significantly changes the aluminium deposition/stripping peaks. For example, the addition of acetone results in one big positively shifted reduction peak at 0 V with onset potential at 0.4 V and a small oxidation peak at 0.5 V. Similarly, the addition of acetonitrile results in

small reduction and oxidation peaks at -0.4 and 0.9 V, respectively. With the addition of THF, only one big over-potential deposition peak at -1.5 V and small over-potential stripping peak at 1.2 V are observed. It is noted that the current density of the acetonitrile based solution is almost one order magnitude lower than those of acetone and THF based solutions, indicating the interaction in the former is much stronger than the latter ones. On the other hand, when toluene and DCM are added, reversible aluminum deposition/stripping are well maintained. Also, the addition of toluene and DCM results in current density increase of 13 % and 10 %, respectively. Considering the lower viscosity of DCM (0.44 cP) than that of toluene (0.59 cP), the lower current density in the former might be attributed to the weak interaction of the lone pairs of the chlorine atom in DCM with $AlCl_3$. However, the interaction between the ionic liquid and DCM is much weaker than those between the ionic liquid and acetone, acetonitrile and THF.

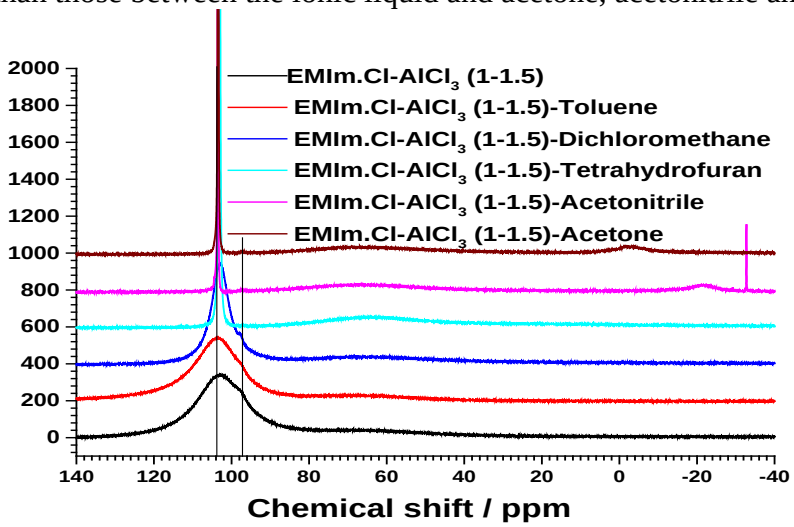

Fig. 24. ^{27}Al NMR spectra of ionic liquid EMImCl-$AlCl_3$ (1-1.5, in molar ratio) and its mixtures with equal volume of different organic solvents

To confirm the interactions, ^{27}Al NMR spectra were obtained for the ionic liquid and its mixtures with different organic solvents. As shown in **Fig. 24**. One broad peak at 103 ppm and an apparent shoulder at 97 ppm for the pure ionic liquid can be assigned to $AlCl_4^-$ and $Al_2Cl_7^-$, respectively.[20-22] No peak change is observed when toluene is added, apparently attributed to the lack of interactions. With the addition of DCM, the spectrum becomes narrower and sharper, and at the same time the signal at 97 ppm decreases due to the weak interaction as mentioned above. However, with the addition of acetone, acetonitrile or THF, the signal at 97 ppm totally disappears, because all $Al_2Cl_7^-$ (or excess $AlCl_3$) are consumed to form complexes with the organic solvents, and as a result new complexation peaks are observed. The above ^{27}Al NMR spectra data are consistent with those of CV data in **Fig. 23** and previous reports on the complexes formed between $AlCl_3$ and organic solvents. [22-25]

The tendency of $Al_2Cl_7^-$ to complex with organic solvents bearing electron lone pairs and the consequent loss of electrochemical activity towards aluminum deposition/stripping deems careful selection of suitable solvents and potential polymer hosts in preparing polymer gel electrolytes for electrodeposition of aluminum. The routine polymers used to prepare polymer gel electrolytes for lithium ion batteries such as polyethylene oxide (PEO), polyacrylonitrile (PAN), polymethyl methacrylate (PMMA), and polyvinylidene fluoride (PVdF) [16, 17] all have

functional groups that are either similar to or stronger than the aforementioned organic solvents. For example, PEO and PAN have the same functional groups as THF and acetonitrile, respectively, while PMMA and PVdF have stronger functional groups than acetone and DCM, respectively. Therefore, they are not good candidates for preparation of polymer gel electrolytes for application in aluminum deposition and rechargeable aluminum ion batteries. Fortunately, there was a recent report on the formation of a low melting eutectic mixture from equal molar acetamide and $AlCl_3$, which could be used for aluminum deposition. [21] Inspired by the report we here exploit the possibility of using a double bond containing analog of acetamide, acrylamide, as the active monomer to prepare polymer gel electrolyte. The complexation of acrylamide with $AlCl_3$, either from acidic EMImCl-$AlCl_3$ ionic liquids or from freshly added $AlCl_3$, will be polymerized in the presence of ionic liquid to obtain polymer gel electrolyte.

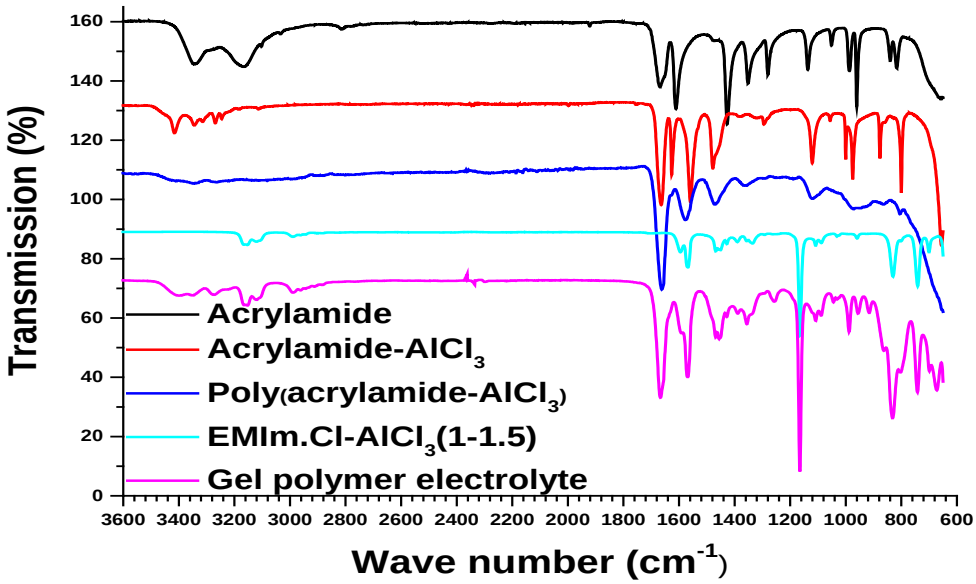

Fig. 25. FTIR spectra of acrylamide, acrylamide-$AlCl_3$(1-1, in molar ratio), poly(acrylamide-$AlCl_3$, 1-1 in molar ratio), EMImCl-$AlCl_3$ (1-1.5, in molar ratio) and polymer gel electrolyte based on poly(acrylamide-$AlCl_3$, 1-1 in molar ratio) containing 80wt% EMImCl-$AlCl_3$ (1-1.5, in molar ratio).

The complexation between acrylamide and $AlCl_3$ can be clearly observed by analysis of the IR spectra. As shown in **Fig. 25**, the N–H stretching frequencies are shifted from 3350 and 3160 in pure acrylamide to 3420 and 3340 cm^{-1} in the complexed mixture.[26] The C-N stretching frequency and the NH_2 scissoring frequency are shifted from 1420 and 1350 to 1480, and 1450 cm^{-1}, respectively.[26] Similarly, the C=O, C=C and C-C stretching frequencies are shifted from 1670, 1650 and 1605 to 1660, 1622 and 1560 cm^{-1}, respectively. [26] These frequency shifts are clearly due to the complexation of the electron-starving $AlCl_3$ with the oxygen from the amide that are delocalized through the C=C double bond and the NH_2 group. For the IR spectra of the polymerized complex from acrylamide and $AlCl_3$, poly(acrylamide-$AlCl_3$), the apparent change is the disappearance of the double bond due to the polymerization. As for the spectrum of the polymer gel electrolyte containing 80 wt% ionic liquid, it clearly combines the feature from both poly(acrtylamide-$AlCl_3$) and the acidic ionic liquid. A typical picture of the polymer gel electrolyte containing 60 wt% of ionic liquid is shown in **Fig. 26**.

Fig. 27 shows the ionic conductivities of the polymer gel electrolytes containing different amount of ionic liquid. Since pure poly(acrylamide-$AlCl_3$) is a fragile solid, its conductivity was not measured. In addition, the gel electrolytes containing less than 50 wt% of ionic liquid were not prepared because of the expected low ionic conductivities. As shown in **Fig. 27**, at 20 ^oC the ionic conductivities of the polymer electrolytes containing 50, 60, 70, and 80 wt% of ionic liquid are 5.29 x 10^{-5}, 2.00 x 10^{-4}, 8.87 x 10^{-4}, 1.66 x 10^{-3} S cm^{-1}, respectively. Usually, an ionic conductivity above 10^{-3} S cm^{-1} is good enough for practical applications. Also, if needed, high temperature can be utilized to achieve higher ionic conductivities. For example, the ionic conductivity of the polymer gel membrane with 80 wt% ionic liquid at 50 ^oC is 3.62 x 10^{-3} S cm^{-1}, more than double that at 20 ^oC.

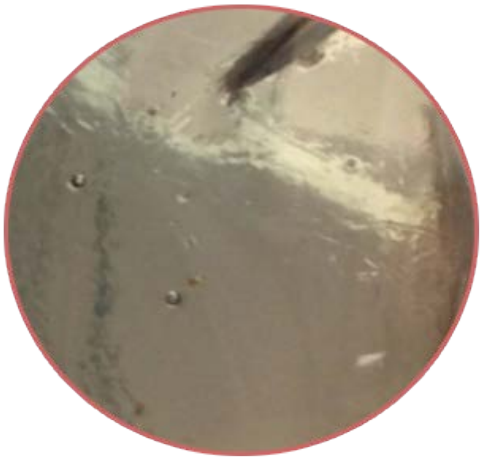

Fig. 26. Pictures of the membrane containing 60 wt% of (a) $AlCl_3$-EMIm.Cl.

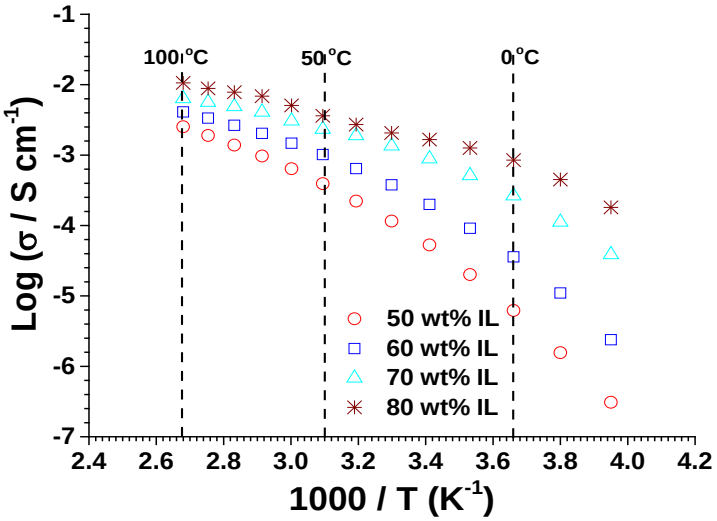

Fig. 27. Temperature dependence of ionic conductivities of the gel polymer electrolytes based on polyacrylamide containing different amount of EMImCl-$AlCl_3$ (1-1.5, in molar ratio)

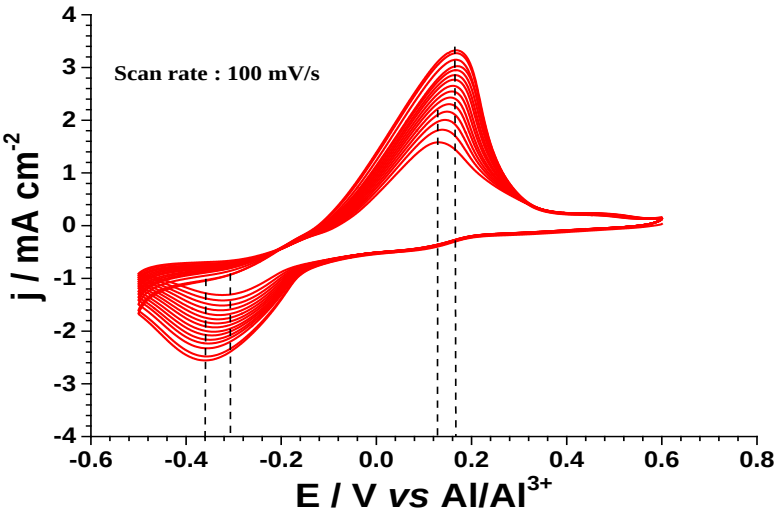

Fig. 28. Cyclic voltamograms of the electrolyte containing 60 wt% of EMImCl-$AlCl_3$ (1-1.5, in molar ratio) at 50 ^oC at a scan rate of 100 mV/s. Cu and Al plates were used as working and counter electrode, respectively.

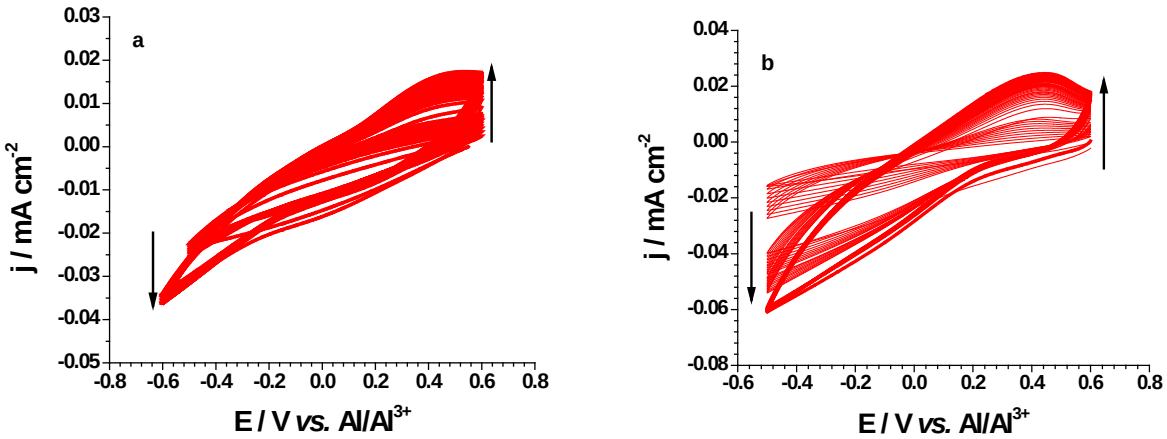

Fig. 29. Cyclic voltamograms of the membrane containing 60 wt% of a) $AlCl_3$-4-propylpyridine (1.4:1) and b) $AlCl_3$-acetamide (1.2:1) at 40 ^oC. Scan rate: 100 mV/s. Cu and Al plates were used as working and counter electrode, respectively.

Fig. 28 shows the CVs of the polymer gel electrolyte with 60 wt% of ionic liquid on a Cu working electrode at a scan rate of 100 mV/s at 50 ^oC. The electrolyte exhibited a well-defined Al deposition/stripping peaks during the initial CV scan. It is noticed that the current densities increase with increasing scan cycles, indicating an activation process, probably due to the gradual removal of the residual surface oxide on the Al plate. In addition, it is also noticed that both the cathodic peak and anodic peak shift with cycling, that is, they shift from initial -300 mV and 130 mV to -360 mV and 170 mV after 15 cycles, respectively. This might be related to the fact that the same aluminum plate was used as both counter and reference electrode, on which the surface oxide layer being removed successfully with cycling as evidenced by the current increasing with cycling. Anyway, this is the first example of electrolyte showing reversible Al deposition and stripping. There is an additional reduction peak observed at 0.1 V, which might be due to the reduction of residual double bond (acryl group) within the membrane. In addition,

polymer gel membranes containing 60wt% of $AlCl_3$-4-propylpyridine (1.4:1) and $AlCl_3$-Acetamide (1.2:1) were also prepared and the corresponding CVs were shown in **Fig. 29a & b**, respectively. The deposition and stripping peaks of Al were observed in both membranes. However, the current densities were much smaller than that based on $AlCl_3$-EMIm.Cl mixture, mainly due to the intrinsic lower ionic conductivities of the latter two membranes.

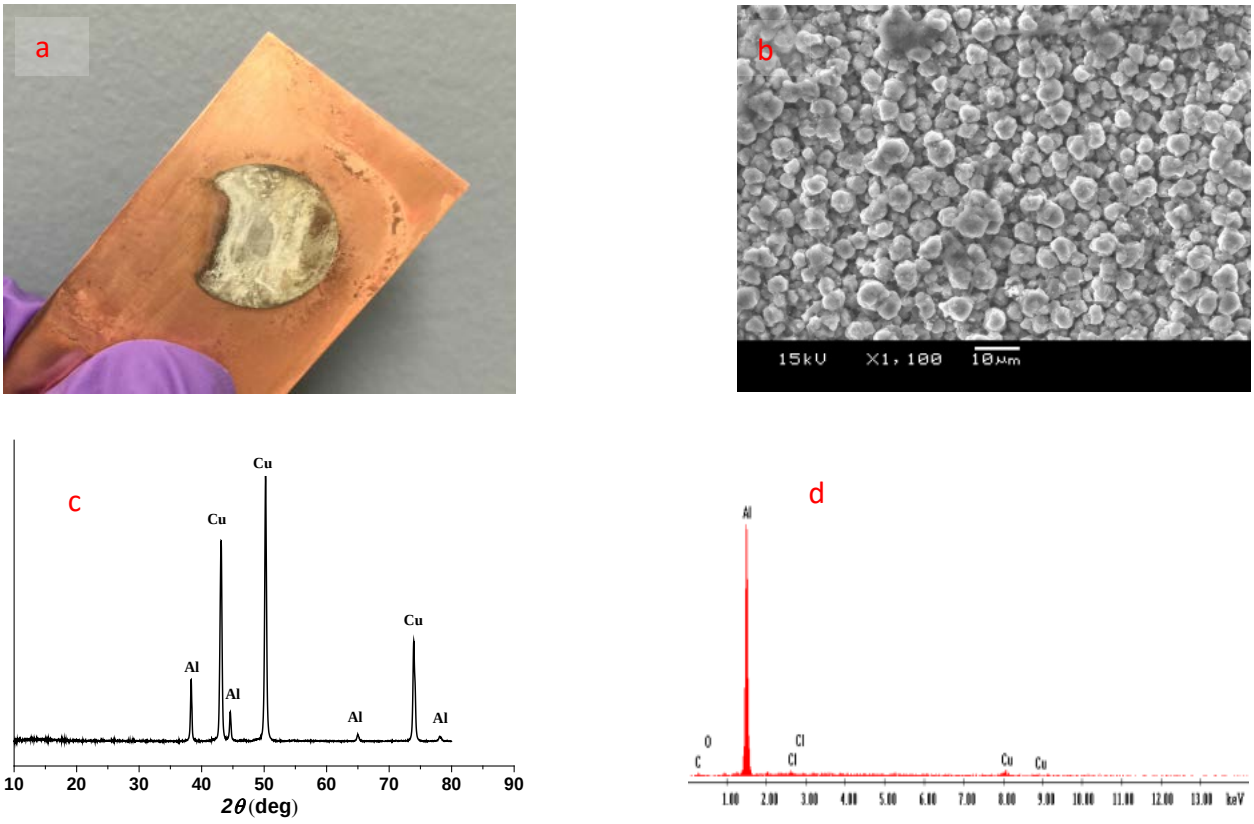

Fig.30. Digital image (a), scanning electron micrograph (b), X-ray diffraction pattern (c), and energy-dispersive X-ray spectroscopy analysis (d) of the electrodeposited aluminum on copper substrate.

To check the possibility of electroplating Al using this new polymer gel electrolyte, a constant voltage of -300 mV was applied at 50 °C for 4 hours, with copper plate as the working electrode and Al as both counter and reference electrode. **Fig. 30a** shows that the Cu substrate is covered by an off-white deposit (yellowish) after the electrodeposition, even though the deposition seems not homogeneous and some part of the depots has been removed during post-deposition cleaning. A SEM image (**Fig. 30b**) shows fine grain-like Al crystals. The relatively large crystal size is related to the low initial current density, as compared with those from liquid electrolytes,[27, 28] [28] resulting in fewer crystal seeds. To confirm the purity of the deposition, the film was further analysed with x-ray diffraction and energy–dispersive x-ray spectroscopy. As shown in **Fig. 30c and d**, there are only signals of the substrate copper and the deposited aluminum.

3.3 Electrodeposition of aluminum using ionic liquid bath

In parallel to the effort of development of new ionic liquid at ORNL, electrodeposition of aluminum was also performed at UM inside nitrogen filled glovebox using three-compartment cell with treated substrates (either Cu or carbon steel) as the working electrode, Al rod as the counter electrode and Al wire as reference electrode. The purpose is to evaluate and optimize the parameters affecting electrodeposition of aluminum. The parameters such as current density, use of co-solvent, influence of current on/off duration for pulsed current plating method, and anodization time are evaluated and optimized, respectively. The ionic liquid used for parameter optimization is the acidic mixture of 1-ethyl-3-methylimidazolium chloride and $AlCl_3$ in a molar ratio of 1:1.5.

3.3.1 Influence of current density

The electrodeposition was carried out using constant current method until the accumulated charges reached 100C. **Fig. 31** a & b shows the micrographs of the electrodeposited Al on Cu under the current density of 3.8 and 2.5 mA cm^{-2}, respectively. The decrease of current density results in a progressive increase in the grain size which is attributed to the high overpotential associate with decreasing current density. The high potential increases nucleation rate and increases the free energy for formation of new nuclei and refine the grain size. But we can see at lower current density, the structure of deposited Al layer looks looser and cracked than those at higher current density.

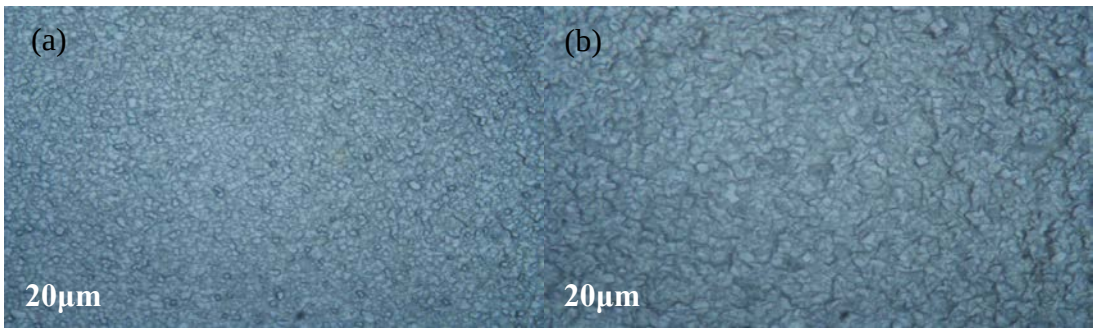

Fig. 31. The Microscopes of electrodeposited Al on Cu at different current density (a) 3.8mA/cm^2, (b) 2.5mA/cm^2.

Fig. 32 shows complex plane impedance plots of different current density Al coatings on steel. The parameters obtained by modeling of electrochemical impedance spectroscopy (EIS) data. The data reveals that the highest polarization resistance (Rp) was obtained at higher current density (5.1mA/cm^2) and a trend of decreasing current density with decreasing Rp. The result indicates that increasing current density causes the higher overpotential. This overpotential increases nucleation rate by increasing the free energy for formation of new nuclei that is helpful to refine the grain size and form compact structure of Al deposits. Because in corrosion behavior, if the structure of coating (film) is loose and porous on the substrates, it results in lower polarization resistance (Rp) and makes the electrolyte (such as, NaCl, O_2 and H_2O) easier to penetrate between the coating and substrate, causing deterioration of the passivity quickly and bad adhesion properties. Furthermore, **Fig. 32** shows that polarization resistance of the Al

deposits obtained under the higher current densities (5.1 and 3.8 mA/cm^2) are much higher than those obtained under lower current densities (2.5 and 1.3 mA/cm^2).

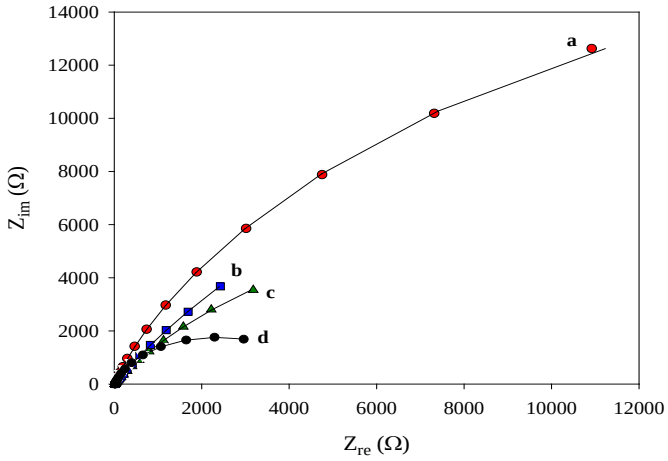

Fig. 32. EIS of Al coatings on steel under different current densities (a) 5.1 (b) 3.8 (c) 2.5 (d) 1.3 mA/cm^2 in 3.5wt% NaCl solution. Solid line is the Randles-Ershler model.

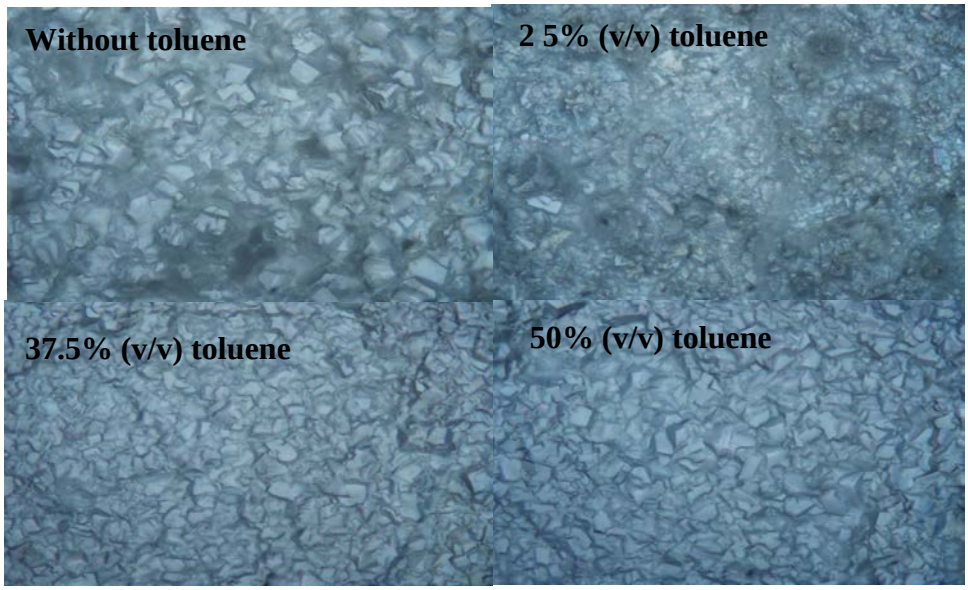

Fig. 33. Optical micrographs of electrodedeposited Al on carbon steel (3.82 mA cm^{-2} and 100 C) as a function of toluene content. All current efficiency are close to 100%.

3.3.2 Influence of co-solvent

Fig. 33 shows the micrograpies of electrodeposited Al on steel plates using eutectic mixture of EMIm.Cl-$AlCl_3$ (1-1.5 by molar) containing different amount of toluene as co-solvent. When 25% (v/v) toluene is added, the film is uniform, even worse than that without toluene. However, when toluene is increased to 37.5 and 50%, the films are very smooth and dense. The difference

can be attributed to the fact that the addition of toluene decreases the viscosity of the ionic liquid, allowing the nucleation grows much smoother. The corrosion resistance of the Al-coated steel plate with and without toluene was evaluated by electrochemical impedance spectroscopy (EIS) and potentiodynamic polarization measurement (pitting test) in 3.5 wt% NaCl solution. **Table 1** shows that the lowest corrosion rate (C_{rate}) is the Al film without toluene (39 cm s^{-1}), and the C_{rate} of Al film with 50% toluene (72 cm s^{-1}) is close to that without toluene, which all have very good corrosion resistance for steel. The results indicate that although the corrosion rate of deposited Al on carbon steel doesn't affected by the toluene, the brightness of the Al films increases and they become more adherent. However, for practical plating applications, organic solvents won't be used due to their toxicity and environmental concerns.

Table 1. Parameters from PDP experiments

Toluene % (v/v)	$E_{corr\ (V)}$	β_a (mV)	β_c (mV)	C_{rate}(cm s^{-1}) (x10^{-11})
0	-0.74	86.3	303	39.0
25	-1.00	161	350	287
37.5	-0.81	286	298	83.0
50	-0.83	306	302	72.0

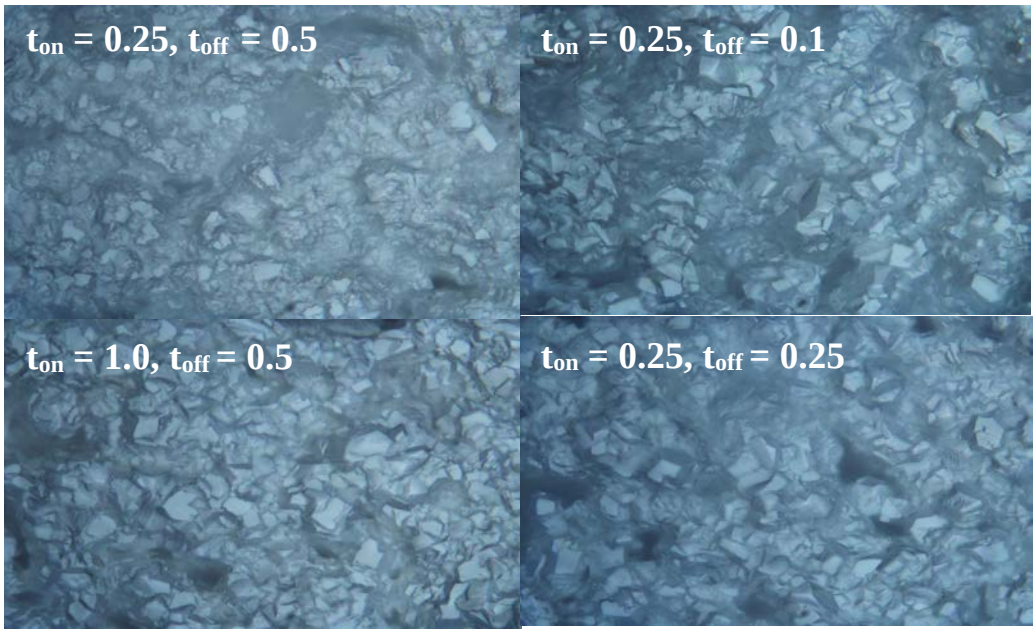

Fig. 34. Optical micrographs of electrodeposited Al on steel using galvanostatic pulse methods at a cathodic current (J_{on}) of 5.1 mA cm^2 and an anodic current density (J_{off}) of 0.32 mA cm^{-2}.

3.3.3 Influence of current on/off duration of pulsed current plating method

Fig. 34 shows that optical micrographics of Al deposited on carbon steel with different current on/off durations at constant cathodic (J_{on} =5.2 mA cm^{-2}) and anodic (J_{off} = 0.32 mA cm^{-2}) current densities. The data reveals that the surface morphologies of deposits change with varying of t_{on} and t_{off}. We can see that the surface become smooth and the grain size of Al film is getting smaller with decreasing t_{on} at fixed t_{off} (t_{off} = 0.5s) and with increasing t_{off} at fixed t_{on} (t_{on}=0.25). This might be due to the fact that high current density under short time (t_{on}) results in thin and smooth monolayer Al film on surface of electrodes. When the anodic current density (J_{off}) 0.32 mA cm^{-2} with t_{off} is applied on the surface of Al film, it removes or dissolves the active (rough) sites of Al film for preferential Al deposition during slight anodic dissolution to make more thin and smooth monolayer Al film layer by layer for the next t_{on} duration. But if the t_{on} is too long, Al particles grow continuously after the initial nucleation process to make rough Al film on the surface of electrode or t_{off} is too short, the removal of the active (rough) sites of the Al film is not enough for preferential Al deposition to make smooth monolayer Al film layer. Therefore, the suitable current on/off duration plays an important role for the improvement of Al coating with pulse plating method.

Table 2. Parameters from fitting EIS data for electrodeposited Al on carbon steel under constant cathodic and anodic current densities to the FCC model.

(t_{on}, t_{off})/s	*R_s / (Ω)*	*Q^n/ (10^5F s^{n-1})*	*R_{pore} /(Ω)*	*n*	*R_{ct} (Ω) (x 10^4)*
(0.25,0.5)	12.54	1.1	41.24	0.7892	17070
(0.5,0.5)	12.26	3.6	3371	0.936	6271.0
(1,0.5)	11.67	8.0	129.4	1.000	7449.0
(0.25,0.25)	12.78	2.9	4336	1.000	3795.0
(0.25,1)	12.66	1.1	40.87	0.9414	6489.0

Table 3. Corrosion rates from potentiodynamic polarization experiments.

(t_{on}, t_{off})s	*$E_{corr\ (V)}$*	*β_a (mV)*	*β_c (mV)*	*C_{rate} (cm s^{-1}) (x10^{-11})*
(0.25,0.5)	-0.734	93.8	386.2	2.08
(0.5,0.5)	-0.755	92.2	386.7	3.87
(1,0.5)	-0.761	154.5	488.1	7.6
(0.25,0.25)	-0.75 0	93	399.3	4.6
(0.25,1)	-0.760	73.5	279.6	4.47

Fig. 35a shows that complex plane impedance plots of Al on carbon steel with different current on/off (t_{on}/t_{off}) at constant cathodic (J_{on} =5.2 mA cm^{-2}) and anodic (J_{off} = 0.32 mA cm^{-2}) current densities in 3.5 wt% NaCl solution. The data reveals that the highest polarization resistance (Rp) was obtained at t_{on} = 0.25s and t_{off} =0.5s and a trend of increasing t_{on} with

decreasing polarization resistance (Rp). Fitting of the failed coating circuit (FCC) model reveals that the highest polarization resistance (Rp =17070) in 3.5 wt% NaCl solution was obtained at t_{on}=0.25 and t_{off} =0.5 s duration, among all others current on/off durations (All parameters from **Table 2**). In addition, we can use the Potentiodynamic polarization (PDP) text as shown in **Fig. 35b** to get β_a and β_c tafel slope to calculate the corrosion rate (C_{rate}) using the following equations:

$$R_{pr} = \beta_a \bullet \beta_c / 2.3 (\beta_a + \beta_c) \bullet i_{corr} \quad (1)$$

$$C_{rate} = Mi_{corr} / nF\rho \quad (2)$$

Where R_{pr} is polarization resistance, β is Tafel slope, M is atomic weight, n is electrons transferred, F is Faraday constant and ρ is metal density, respectively. If the corrosion rate is small, it means that the corrosion resistance is better. **Table 3** shows that the best C_{rate} (2.0 cm s^{-1}) is the Al film at t_{on} = 0.25s and t_{off} = 0.5s duration at constant cathodic and anodic current densities.

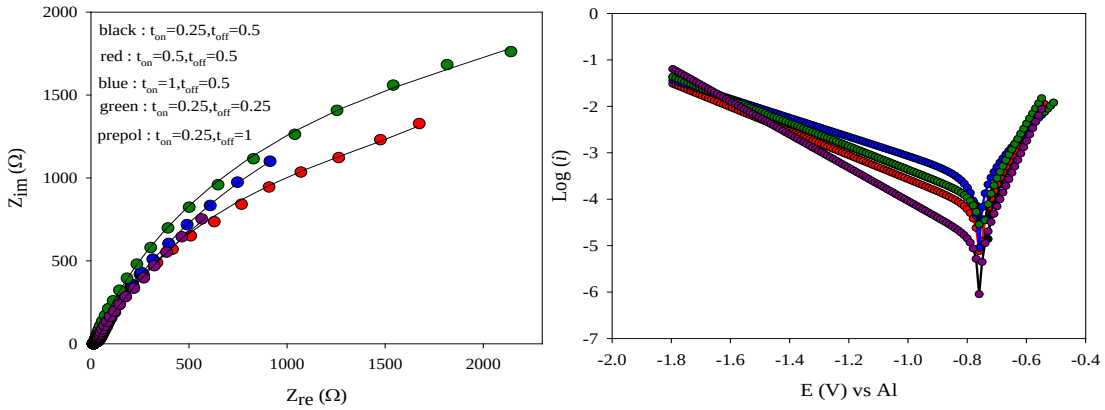

Fig. 35. (a) EIS and (b) Potentiodynamic polarization plots of Al films with different current on/off duration at constant cathodic (J_{on} =5.1 mA cm^{-2}) and anodic (J_{off} =0.32 mA cm^{-2}) current densities in 3.5 %wt NaCl. Solid line is the Failed Coating Circuit model.

3.3.4 Influence of anodization time

Anodization has been used as an electrolytic passivation process to increase the thickness of the natural oxide layer on the surface of metals. The above process is usually performed in aqueous acid solutions, either inorganic or organic ones, such as sulfuric acid, chromic acid, oxalic acid, malic acid etc. The key step is anodic dissolution of the metal electrode to increase the surface area that form in-situ metal oxide layers not only to increase resistance for corrosion and wear but also provide better adhesion for paint primers and glues than bare metals. [29] However, anodization in water free acidic ionic liquids is totally different from anodization in aqueous acidic solutions. There is no metal oxide formed on the surface of the electrode because of the absence of water. Therefore, anodization in acidic ionic liquids can only create fresh surface for better electrodeposition, that is, improving adhesion of the coating layer on the surface of the metals.

Although carbon steel is not routinely anodized as other metals such as aluminum, magnesium, titanium, zinc, niobium and tantalum etc., anodization can potentially create fresh surfaces by dissolving trace elements present in the carbon steel such as magnesium, copper. [30] To check the effect of anodization on adhesion of electrodeposited aluminum, carbon steels were anodized for 0.5, 1 and 2 minutes before electrodeposition. The effect of the anodization on the Al deposit on steel substrate was evaluated based on surface morphology and roughness, which were obtained before and after anodization, and after electrodeposition of 100 C of charge. Constant potential plating method with a potentiostat was used for electroplating Al. **Fig. 36** shows that for the three anodization times, there is no noticeable difference in the surface morphology of the steel before and after anodization. In addition, the difference in the roughness of the steel before and after anodization is negligible (**Table 4**).

To further study the effect of anodization and deposition melt on the electroplating of Al on carbon steel, the electrodeposition was performed using: (1) the same melt used for anodization, and (2) fresh melt. The former involved electrodeposition of Al right after anodization. The latter involved cleaning and drying of carbon steel and then electrodeposition in a fresh melt. The same anodization time were used for both studies. Results were compared with Al electrodeposited on un-anodized carbon steel.

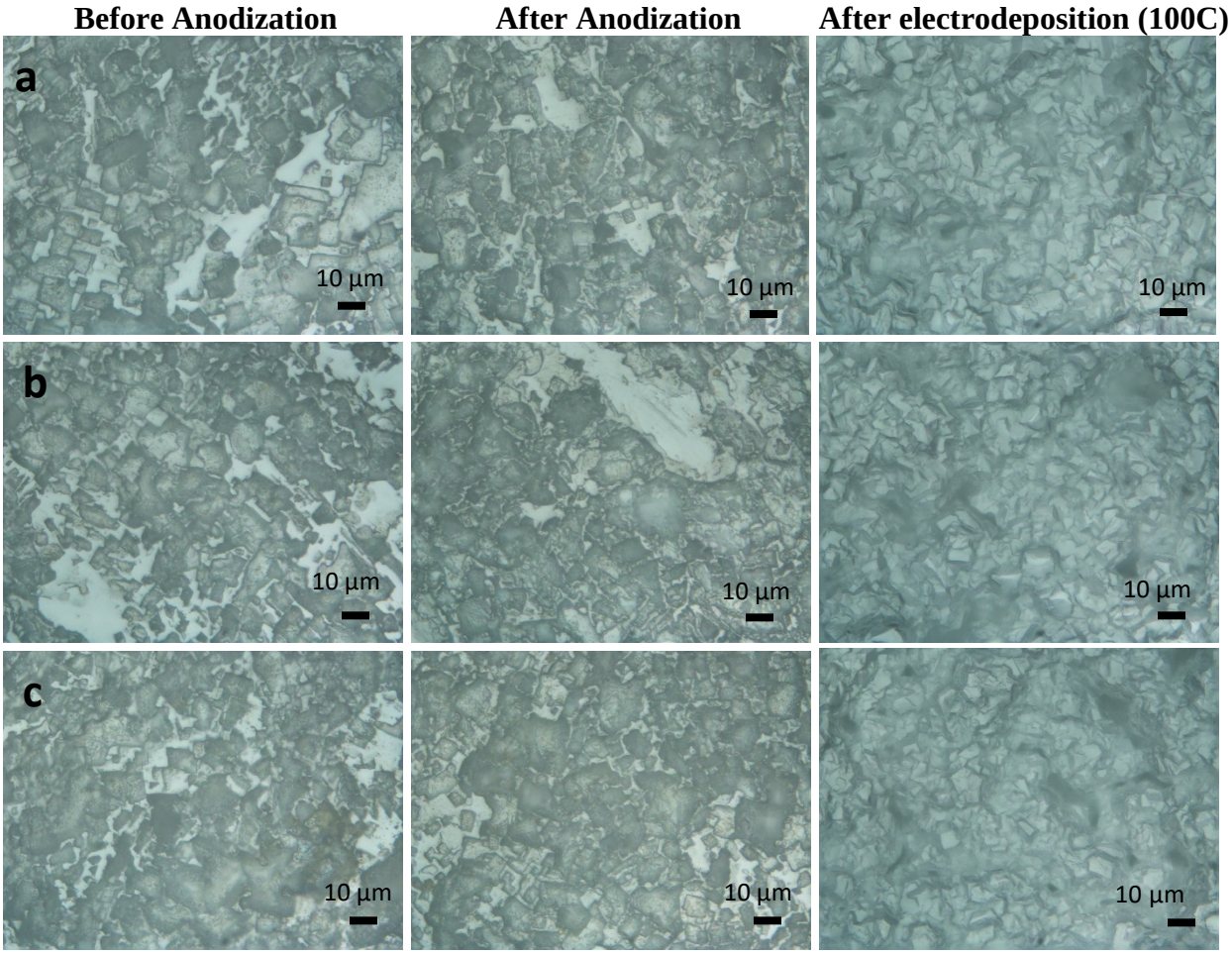

Fig.36. Optical micrograph of carbon steel before and after anodization (first two columns) and Al deposit on steel (third column) for anodization times of (a) 0.5 min; (b) 1 min; and (c) 2 min

Aluminum electrodeposited on carbon steel using fresh melt appeared to have brighter, shinier and a more uniform finish than the Al deposited from the same melt used in anodization (**Figs. 37 and 38**). It is also brighter than the Al deposited on un-anodized carbon steel. Both the tape-and-peel test and the standard ASTM D3359 adhesion tape test showed that deposited Al using anodized and un-anodized carbon steel have good adhesion (**Figs. 39 and 40**).

Table 4. Roughness (nm) of steel before and after anodization (first two columns) and Al deposit on carbon steel (third column) for different anodization times

Anodization Time (min)	Roughness (nm)		
	Before anodization	After anodization	After deposition 100C Al
0.5	1414 ± 38	1289 ± 82	2042 ± 342
1	1680 ± 176	1600 ± 316	1761 ± 111
2	1700 ± 108	1673 ± 239	2092 ± 229

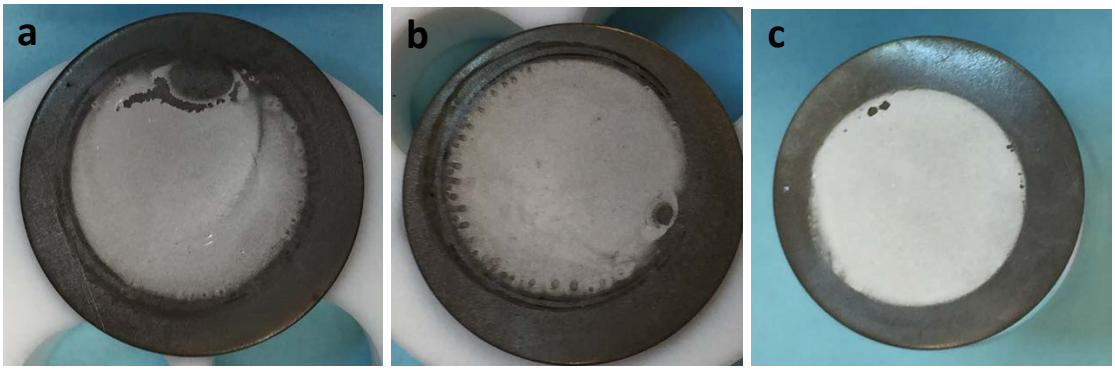

Fig. 37. Photograph of Al electrodeposited on: (a) un-anodized carbon steel; and anodized carbon steel using (b) same melt used in anodization and (c) fresh melt.

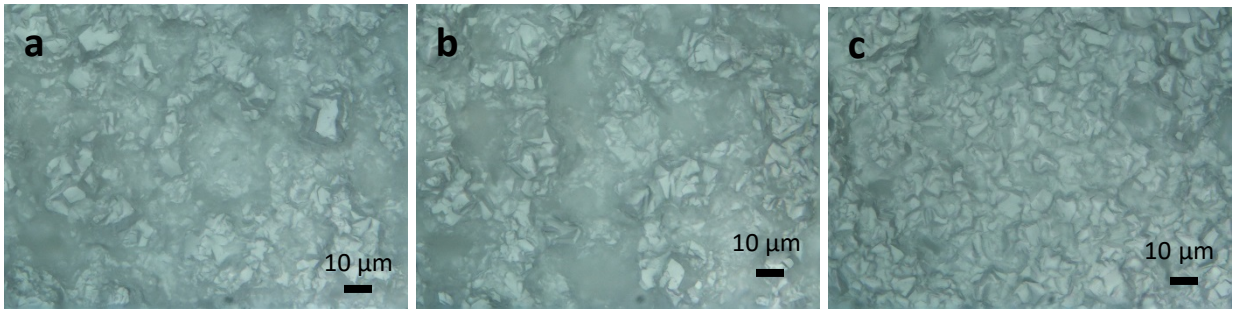

Fig. 38. Optical micrograph of Al electrodeposited on: (a) un-anodized carbon steel; and anodized carbon steel using (b) same melt used in anodization and (c) fresh melt.

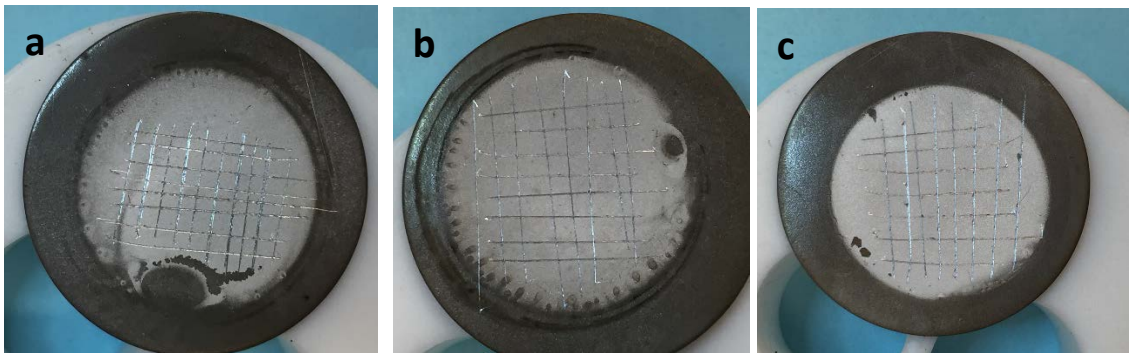

Fig.39. Photograph of Al on carbon steel after ASTM D3359 adhesion tape test. The Al film were electrodeposited on: (a) un-anodized carbon steel; and anodized carbon steel using (b) same melt used in anodization and (c) fresh melt.

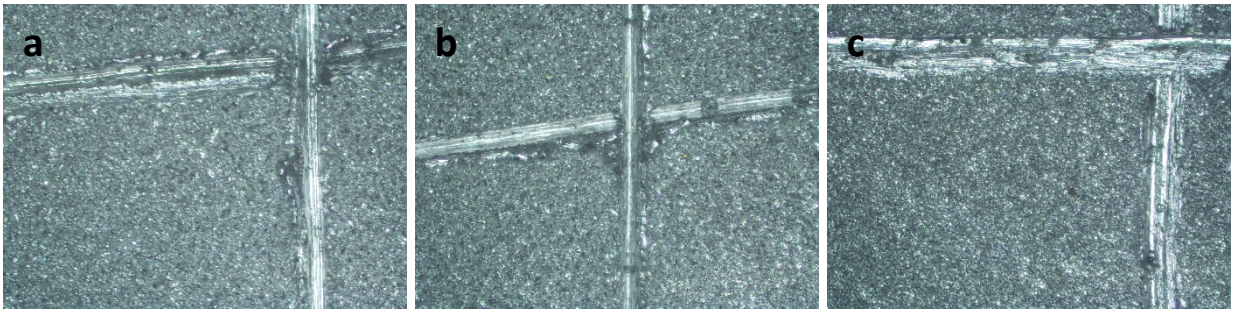

Fig. 40. Optical micrograph of Al electrodeposited on: (a) un-anodized carbon steel; and anodized carbon steel using (b) same melt used in anodization and (c) fresh melt.

3.4. Electrodeposition of aluminum using portable aluminum deposition system (PADs)

Even though the polymer gel membranes can be conveniently used for electroplating of aluminum, they still need to be packed carefully before being used. As a comparison, if the ionic liquids were sealed inside a chamber, it can be used more conveniently. Therefore, a portable plating brush is fabricated as illustrated in **Fig. 41**. The device is made from plastic or glass tubing with an outer layer for inert gas protection. The brush was made by inserting a short length of fiberglass rope into the end of the tube to obtain a brush-type tip. A suitable amount of the $AlCl_3$-EMIm.Cl ionic liquid was added into the barrel/reservoir of the brushes, which soaked into the rope by capillary action. No ionic liquid leaks from the brush if a certain high-density rope is used and care is taken to not loading too much liquid electrolyte. The anode is a large spiral of high purity aluminum wire (1mm diameter) that is forced into the end of the rope inside the barrel of the brush. Electrodeposition of Al or aluminum alloys are performed using PADs and related parameters are optimized, either using a conventional potentiostat instrument or a simple 1.5V D cell battery.

3.4.1. Electrodeposition using a potentiostat instrument

3.4.1.1. Influence of surface treatment

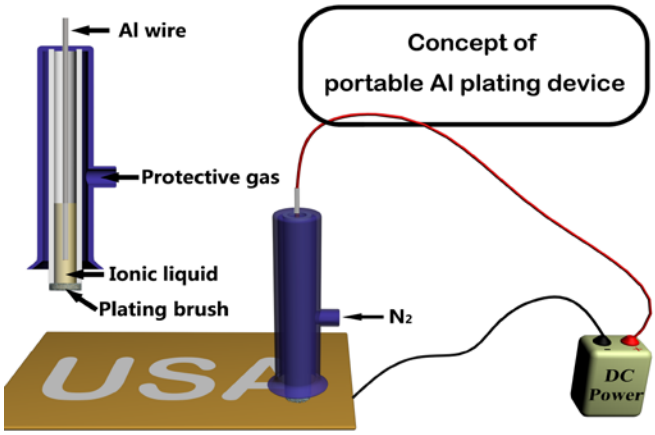

Fig.41. Scheme of portable Al plating device.

Electrodeposition of Al is easier on Cu than on carbon steel. Al has more affinity towards Cu than for Fe and deposition on steel is more difficult. Therefore, it is necessary to find the best method for pre-treatment of the steel surface prior to electrodeposition. Four methods of surface pre-treatment of steel were investigated in this study. The first three used acids for pickling the steel. All four methods used the following surface treatment. Carbon steel were degreased by sonicating it in 2-propanol and then rinsed with copious amount of distilled water. Then, the steel samples were polished successively with SiC emery paper from 320 to 4000 grit. Afterwards, the steel samples were rinsed with distilled water. The samples were then subjected to the different pre-treatment methods described in **Table 5**.

Table 5. Surface pre-treatment methods for carbon steel

Method A	The steel samples were pickled in 10% HNO_3 and rinsed with distilled water. The samples were sonicated in 2-propanol and dried in the glove box vacuum chamber overnight.
Method B	The steel samples were pickled in 10% HCl and rinsed with distilled water. The samples were sonicated in 2-propanol and dried in the glove box vacuum chamber overnight.
Method C	The steel were pickled in a solution of 25% HNO_3 and 50% ethanol and rinsed with distilled water. The samples were sonicated in 2-propanol and dried in the glove box vacuum chamber overnight
Method D	After polishing, the steel were sonicated in 2-propanol and dried in the glove box vacuum chamber overnight. The samples were then polished with 4000 grit SiC emery paper inside the glove box, dipped in dry acetonitrile and wiped thoroughly with KimWipes.

Table 6. Roughness (nm) of steel after surface pre-treatment

Method	*Roughness (nm)*
A	4589 ± 635
B	170 ± 38
C	2547 ± 425
D	321 ± 37

Optical micrograph and stylus profilometer roughness data show that methods B and D produce smoother deposits than methods A and C (**Fig.42** and **Table 6**). The first three methods (A, B, and C) resulted in low plating current density (< 2 mA) so that the full electrodeposition process was not performed. It would take a very long time to deposit a thick Al film with these carbon steel samples. Hence, there is no thickness data from these methods. Method D resulted in the highest current density (~1.9 mA/cm^2). The Al deposit from method D was evaluated for adhesion and thickness. Adhesion was evaluated using classical tape-and-peel test and the standard ASTM D3359 adhesion tape test (**Fig. 43**). Both tests showed that the Al film has good adhesion.

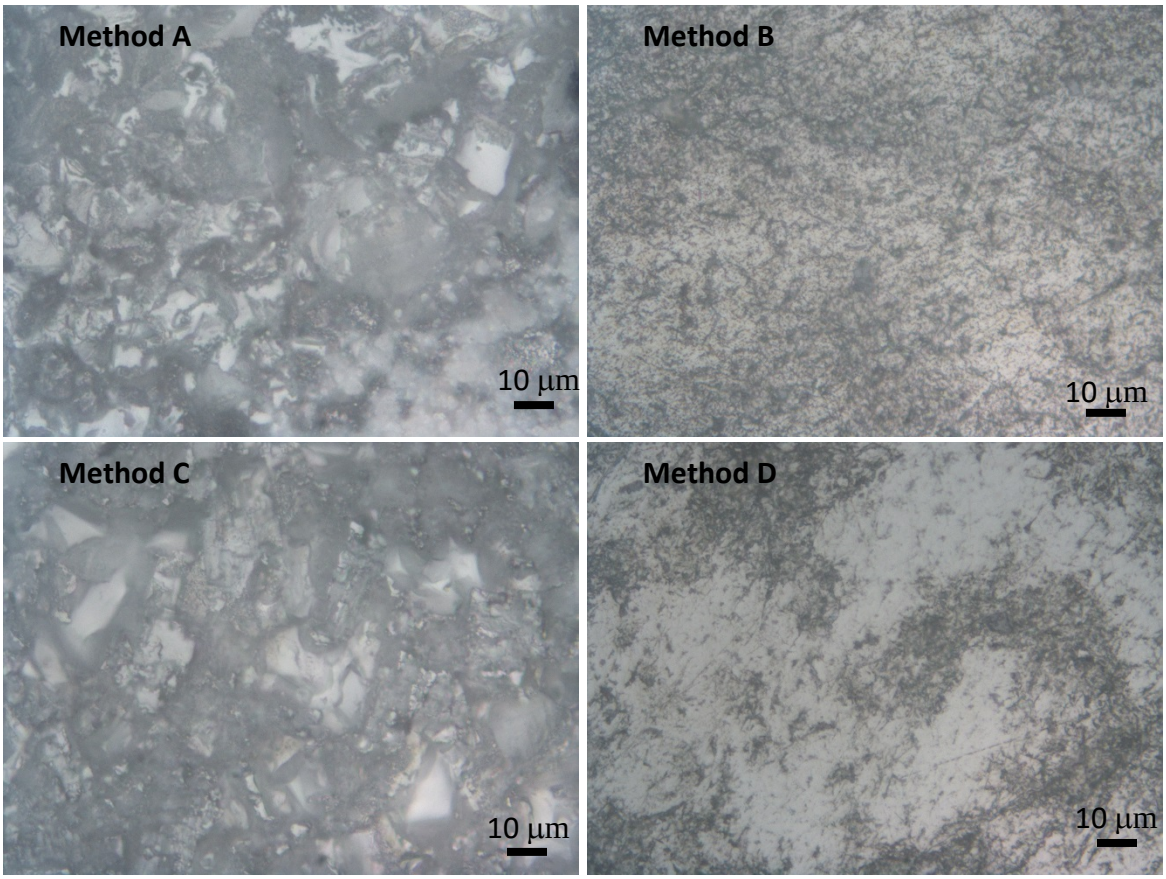

Fig. 42. Optical micrograph of electrodeposited Al on carbon steel prepared using different surface pre-treatment method prior to electrodeposition; 1000x magnification.

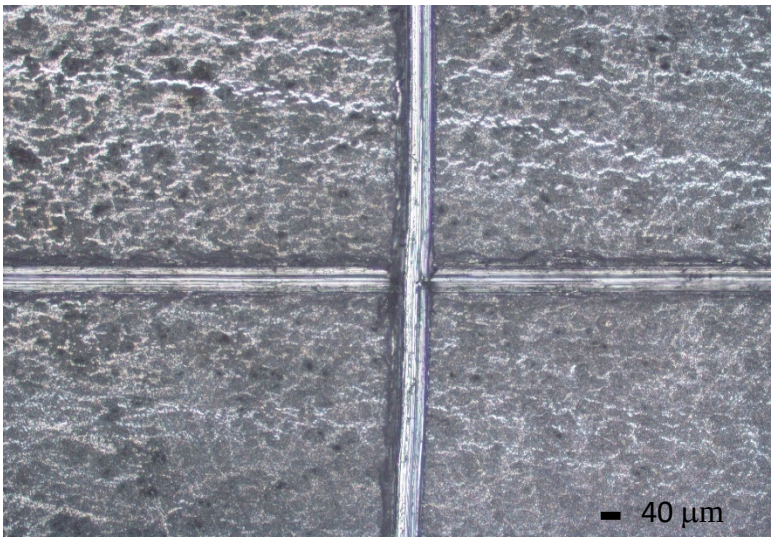

Fig. 43. Optical micrograph of electrodeposited Al on carbon steel subjected to adhesion test; 1000x magnification.

Another carbon steel with an area of 2.0 cm^2 was subjected to method D surface pre-treatment. A charge of 29 C Al film was used to electrodeposit on the surface using constant a potential of 1.5 V. The theoretical thickness of the Al film should be at 5 μm. The cross-section of the resulting electrodeposited Al film was at around 5 μm as shown in **Fig. 44**.

3.4.1.2. Influence of electrodeposition protocol - constant current *vs.* constant potential

Previously, our research was focused on electrodeposition of Al and Al-Mn film on Cu and mild steel using constant current plating method. It was observed that the potential is not stable during the deposition. Recently, we've employed constant potential plating method for the deposition of Al and Al-Mn film on Cu and carbon steel. A constant potential of -1.5 V was used for the deposition and the current output is relatively stable. The Al and Al-Mn film obtained from constant potential plating method was compared with the Al and Al-Mn deposit obtained from constant current method. A current density of 9.95 mA/cm^2 was used for constant current plating method. The plating time of 30 minutes was used for all depositions.

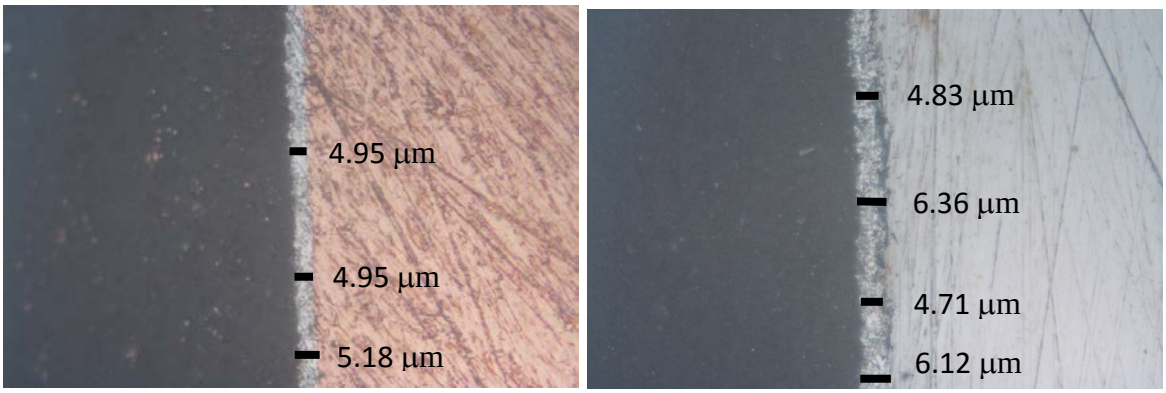

Fig. 44. Cross-section of Al on carbon steel showing the thickness of the deposit; 1000x magnification.

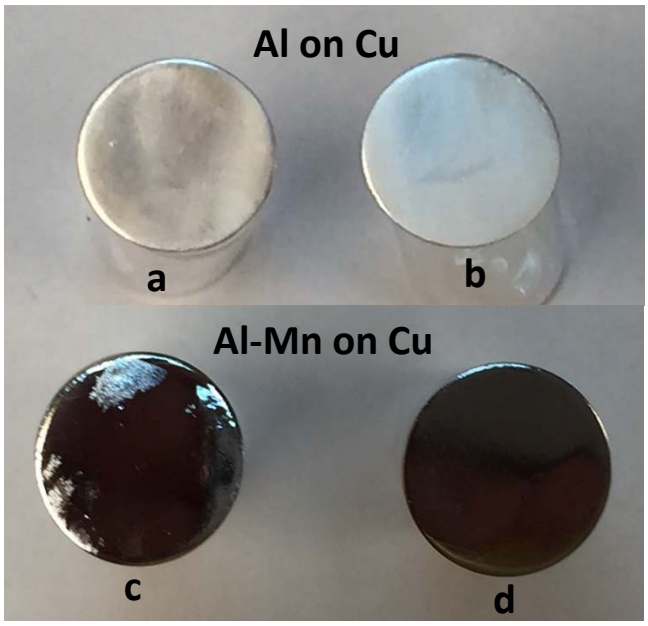

Fig. 45. Photograph of Al (top) and Al-Mn (bottom) electrodeposited on Cu using constant potential (**a** and **c**) and constant current (**b** and **d**) plating method.

Photograph of Al and Al-Mn film on Cu (**Fig. 45**) showed that Al-Mn is shinier and brighter than Al deposit. Both plating methods produced Al-Mn film with mirror finish. The optical micrograph of the Al and Al-Mn film on Cu and mild steel are shown in **Fig. 46**. It can be observed that both plating methods produced smoother Al-Mn film than Al film on both Cu and carbon steel. However, the Al-Mn film looked smoother with constant potential plating method than the constant current method, although surface profiler shows that roughness are relatively the same (**Table 7**). The thickness of the electrodeposited Al was measured by cutting the cross-section of the metal coupon. The thickness of Al on both plating methods are relatively the same (**Fig. 47**).

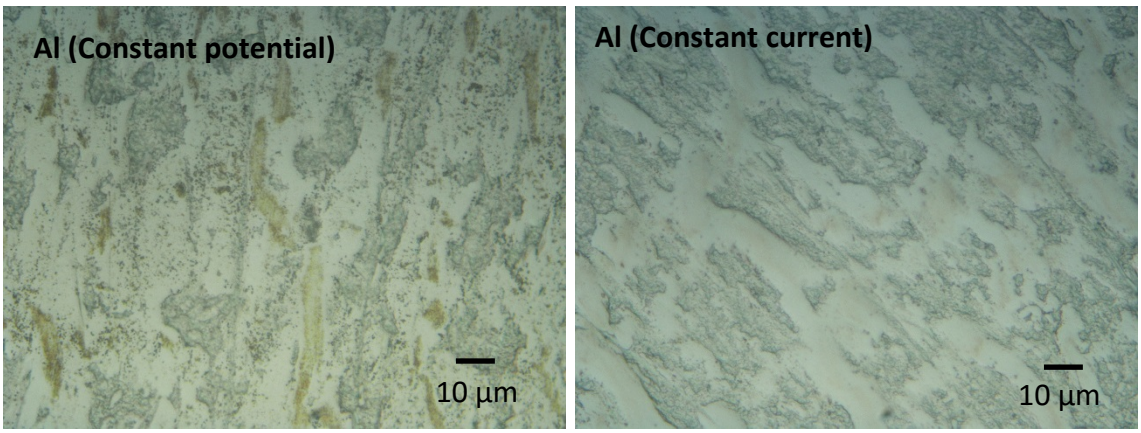

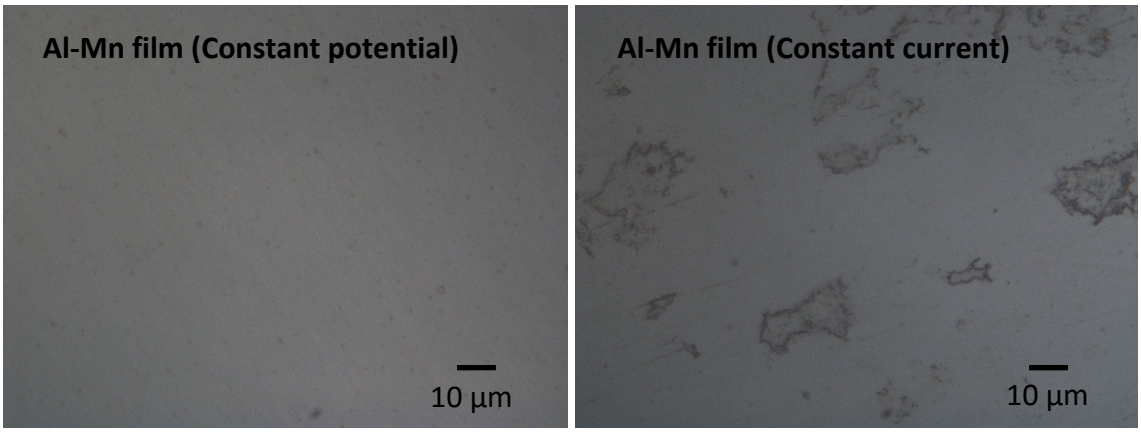

Fig. 46. Optical micrograph of electrodeposited Al and Al-Mn film on Cu using constant current and constant potential (with potentiostat) plating method.

Table 7. Roughness (nm) of Al and Al-Mn film on Cu and carbon steel obtained from a surface profiler.

Metal Substrate	Electroplating method	Roughness of Al (nm)	Roughness of Al-Mn film (nm)
Cu	Constant Current	443 ± 78	115 ± 50
	Constant Potential*	478 ± 250	108 ± 67
	1.5 D Cell Battery	672 ± 104	169 ± 59
Carbon steel	Constant Current	718 ± 48	227 ± 90
	Constant Potential*	1592 ± 156	489 ± 37
	1.5 D Cell Battery	1580 ± 76	959 ± 156

Photograph of Al and Al-Mn film on carbon steel (**Fig. 48**) shows the same trend as that of Al and Al-Mn on Cu. Al-Mn film are shinier and brighter than Al deposit. In addition, the surface morphology shows that Al-Mn film are smoother as shown in the optical micrograph of the deposits (**Fig. 49**). Constant current plating method appeared to produce a smoother Al and Al-Mn film than the constant potential method. This trend is also observed in the roughness data obtained from surface profiler (**Table 7**).

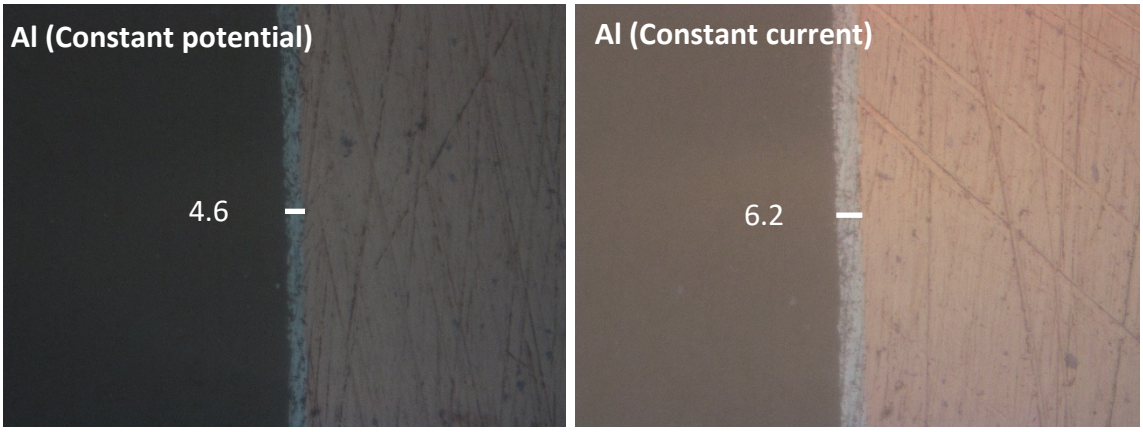

Fig. 47. Cross-section of Al on Cu showing the thickness of the deposit using constant potential and constant current plating method.

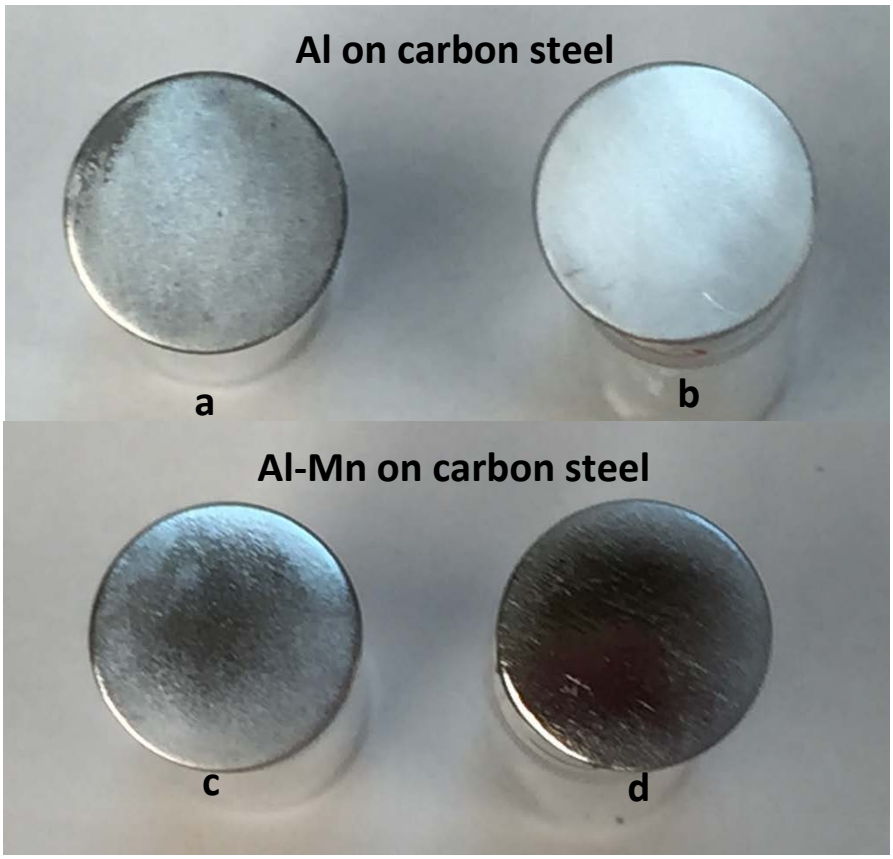

Fig. 48. Photograph of Al (top) and Al-Mn (bottom) electrodeposited on carbon steel using constant potential (**a** and **c**) and constant current (**b** and **d**) plating method.

Cross-section of Al electrodeposited on carbon steel shows that the thickness of Al film are relatively the same for both plating methods (**Fig. 50**). However, the Al deposit from constant current plating method produced a more uniform film than the constant potential plating method.

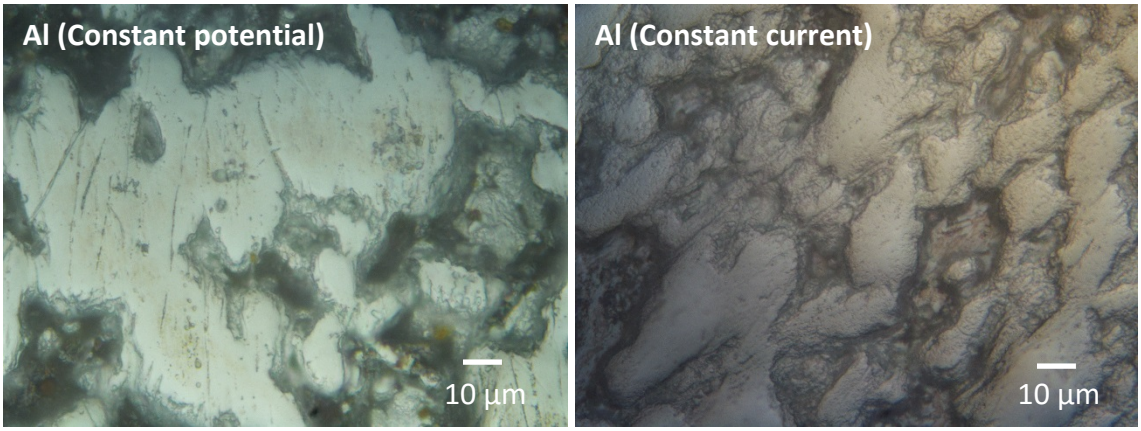

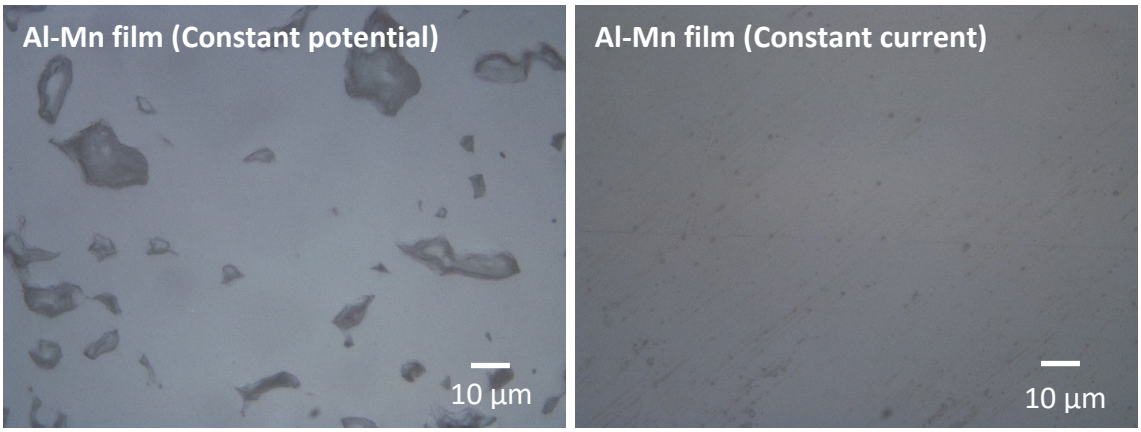

Fig. 49. Optical micrograph of electrodeposited Al and Al-Mn film on carbon steel using constant current and constant potential (with potentiostat) plating method.

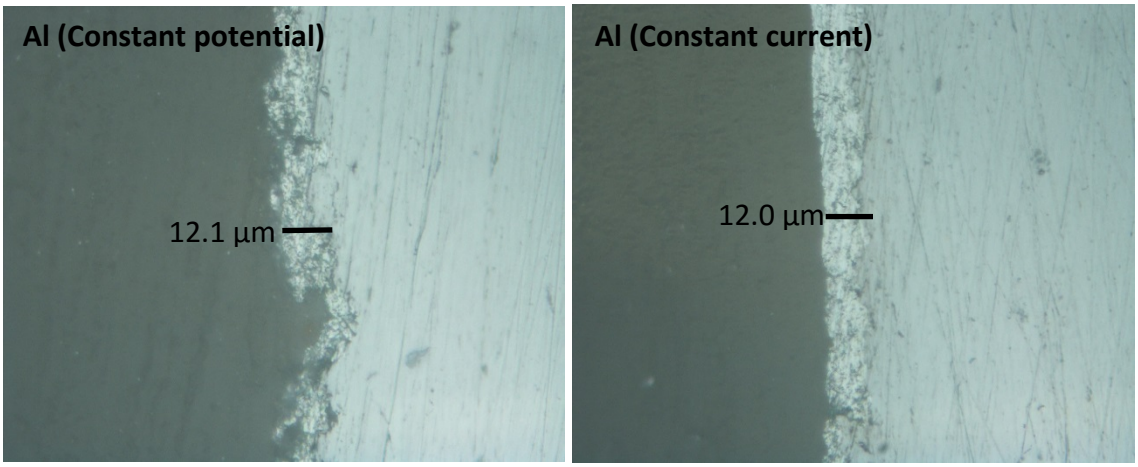

Fig. 50. Cross-section of Al on carbon steel showing the thickness of the deposit using constant potential and constant current plating method.

3.4.2. Electrodeposition of Al using a 1.5 V D cell battery

The electrodeposition of Al and Al-Mn film on Cu and steel were also investigated using constant potential plating method with a 1.5 D Cell battery. The plating time of Al and Al-Mn for Cu and carbon steel were 30 minutes and 60 minutes, respectively.

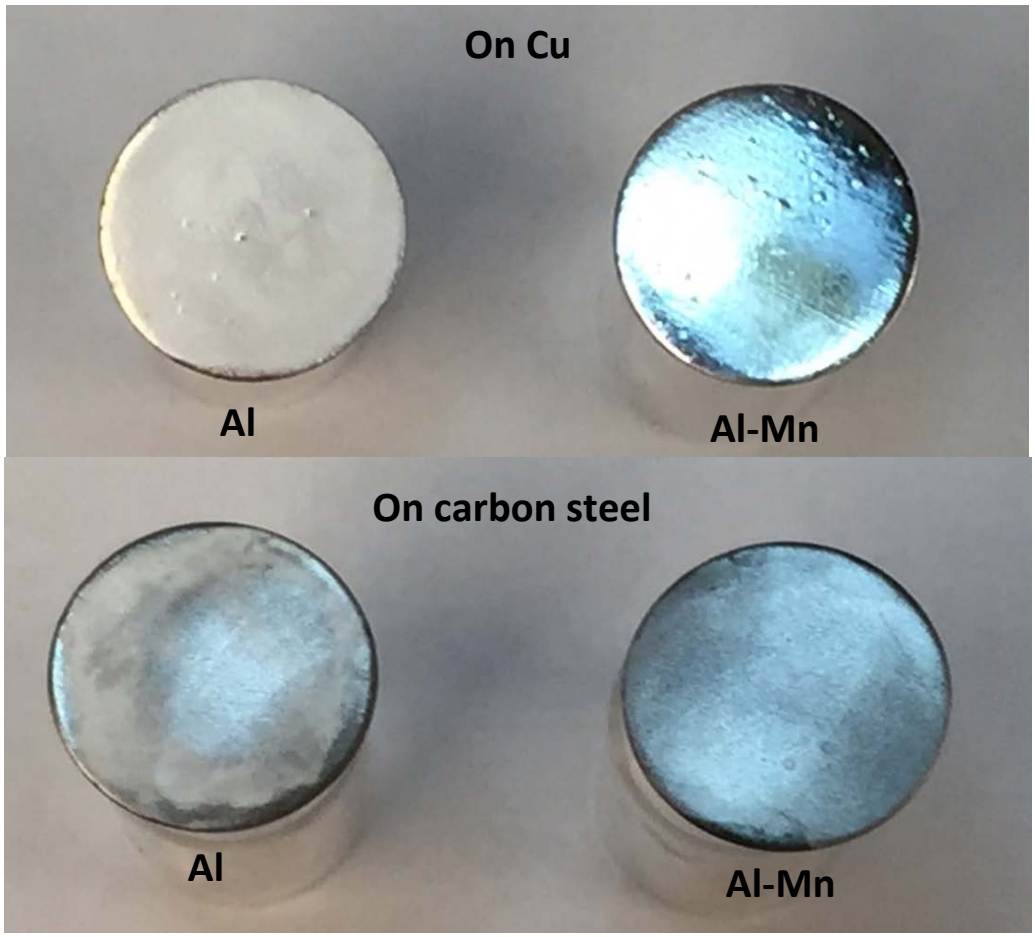

Fig. 51. Photograph of Al and Al-Mn electrodeposited on Cu and carbon steel using constant potential plating method with a 1.5 V D Cell battery.

Photograph shows that Al-Mn film is brighter than Al on both Cu and carbon steel. (**Fig. 51**). The same trend is observed in the surface morphology of the films as shown in optical micrograph (**Fig. 52**). Both constant potential plating methods using potentiostat and 1.5 V Cell battery produced Al and Al-Mn film that have relatively the same surface morphology, roughness and thickness as shown **Table 7**.

The thickness of Al on Cu electrodeposited using constant potential with a potentiostat and a 1.5 D cell battery were relatively the same (**Figs. 47** and **53**). The thickness of Al on steel electrodeposited using a potentiostat with a 30-minute plating time was 12.1 μm. The thickness of Al on steel electrodeposited using a 1.5 D cell battery doubled to 25 μm when the deposition time was doubled to 60 minute.

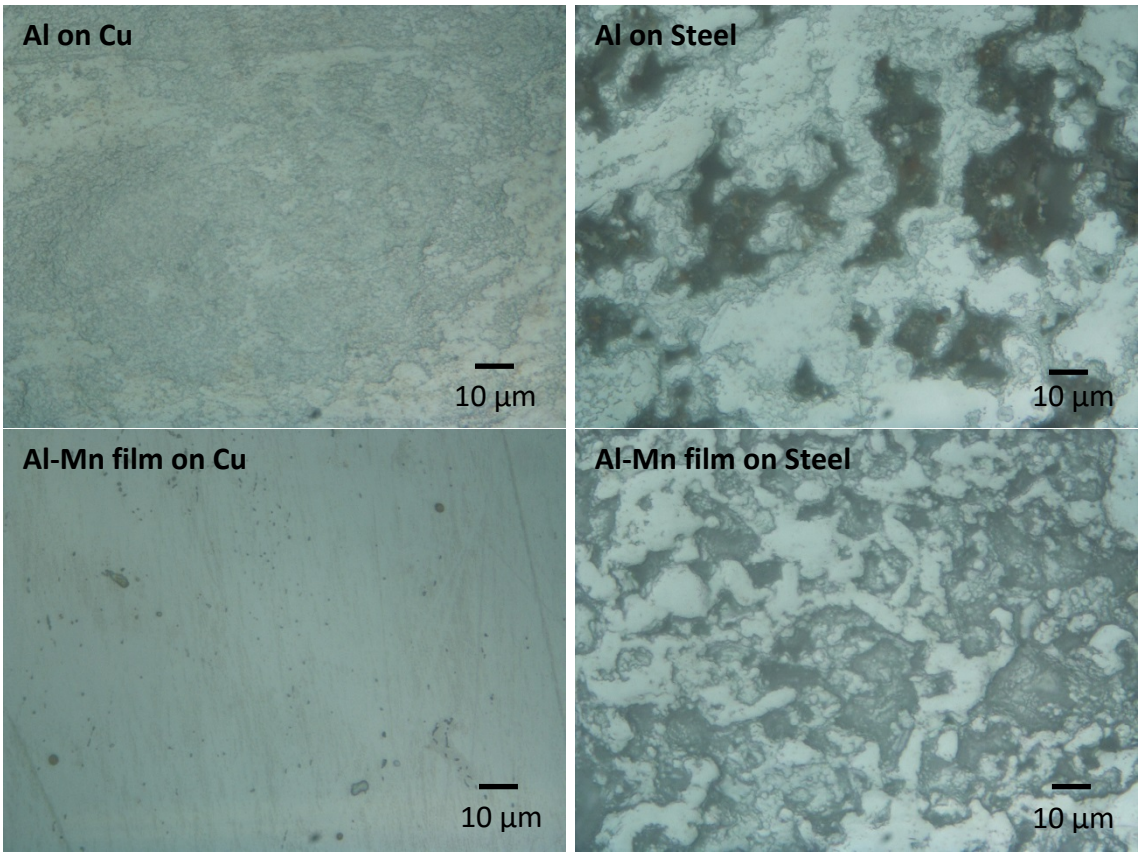

Fig. 52. Optical micrograph of electrodeposited Al and Al-Mn film on Cu and carbon steel using constant potential plating with a 1.5 V D cell battery.

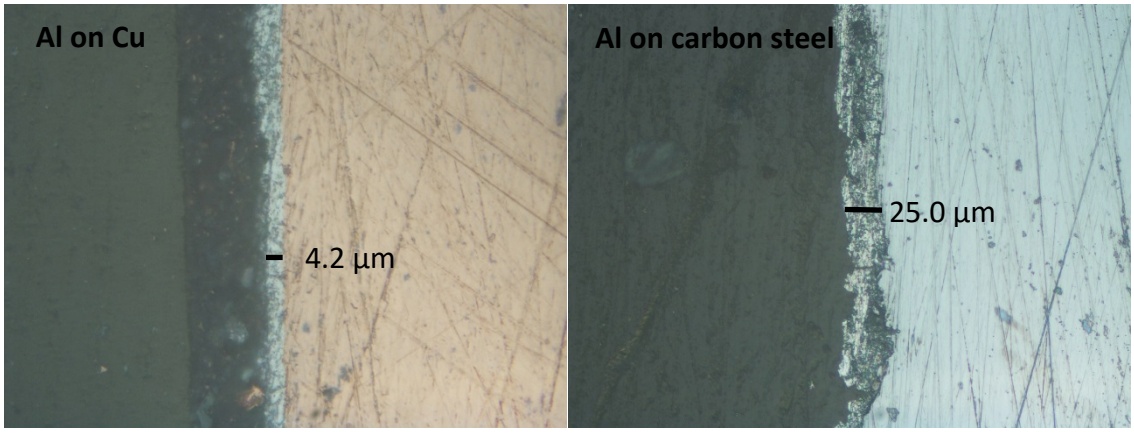

Fig. 53. Cross-section of Al on Cu and carbon steel showing the thickness of the deposit using constant potential plating method with a 1.5 V D cell battery.

4. Conclusions

We have successfully developed new classes of ionic liquids based on the complexation of N, P and S-containing neutral ligands with $AlCl_3$, which can be successfully used for electrodeposition of aluminum. It has been demonstrated that the molar ratio of $AlCl_3$ is important for the electrochemical properties of the ionic liquids. To mitigate the moisture sensitive issues of the $AlCl_3$ based ionic liquids, polymer gel membranes were also successfully developed for the first time, which also exhibited a good electrochemical behavior for the deposition/stripping of Al. It has shown that the selection of functional groups and solvent is crucial in the preparation process of the polymer gel membranes, which will ultimately affect the electrochemical properties of the membranes. It also suggests that the intrinsic ionic conductivity of the ionic liquid will play a key role in the performance of the final polymer gel membrane. Different parameters such as current density, selection of co-solvent, duration of different t_{on} and t_{off} for pulsed current technique, and anodization of the substrate have been optimized for electrodeposition of aluminum. In addition, a portable aluminum plating system (PADs) using an Al-based ionic liquid electrolyte was also successfully prepared for the first time. The process was successfully used to plate Al on Cu or carbon steel substrates. Both a potentiostat instrument and a 1.5 V D cell battery can be used to operate the PADs for aluminum deposition. Al films can be produced after 5 min of plating time, a dense specular film of Al is obtained on Cu or steel. The plating process can also be used to plate aluminum alloy, for example, Al-Mn alloy. Portable plating brush can be used for a wide variety of applications in the defense industry. However, one limitation of the PADs is that it can only be used for electrodeposition on the exposed surface, and can for internal (such as internal surface of a tube) or line of sites.

5. Accomplishment

5.1 Publications

1. C. Wang and C. L. Hussey, Aluminum Anodization in the Low-Melting $LiAlBr_4$-$NaAlCl_4$-$KAlCl_4$ Molten Salt, *ECS Transactions*, 2014, 64 (4) 257-265.

2. L. H. Chou and C. L. Hussey, Corrosion Resistance of Aluminum Films Electroplated on Steel from Chloroaluminate Ionic Liquids Containing Toluene as a Co-Solvent. *ECS Transactions*, 2014, 64 (4) 549-561.

3. Y. X. Fang, K. Yoshii, X. G. Jiang, X. G. Sun, T. Tsuda, S. Dai, Aluminum-based ionic liquid with a neutral pyridine ligand for aluminum electrochemical deposition, *Electrochimica Acta*, 2015, 160, 82-88.

4. C. Wang and C. L. Hussey, Aluminum Anodization in the $LiAlBr_4$-$NaAlCl_4$-$KAlCl_4$ Molten Salt, *J. Electrochem. Soc.*, 2015, 162(3), H151-H156.

5. Y. X. Fang, K. Yoshii, X. G. Jiang, X. G. Sun, S. Dai, New ionic liquids based on the complexation of dipropyl sulfide and $AlCl_3$ for electrodeposition of aluminum, *Chem. Comm.*, 2015, 51, 13286 – 13289.

6. X. G. Sun, Y. X. Fang, X. G. Jiang, K. Yoshii, T. Tsuda, S. Dai, Polymer gel membranes for application in aluminum deposition and rechargeable aluminum ion batteries, *Chem. Commun.*, 2016, 52, 292 – 295.

7. C. Wang, A. Creuziger, G. Stafford, C. L. Hussey, Anodic Dissolution of Aluminum in the Aluminum Chloride-1-Ethyl-3-methylimidazolium Chloride Ionic Liquid, *J. Electrochem. Soc.*, 2016, 163(14), H1186-H1194.

5.2 Patents

1. S. Dai, X. G. Sun, Y. X. Fang, K. Yoshii, "aluminum trihalide-neutral ligand ionic liquids and their use in aluminum deposition" US patent Application Serial No. 14/516,611, filed on October 17, 2014.

2. S. Dai, X. G. Sun, C. L. Hussey, L. H. Chou, "aluminum deposition devices and their use in spot electroplating of aluminum". US patent Application Serial No. 14/516608, filed on October 17, 2014.

5.3 Awards

A R&D 100 award was granted for the portable aluminum deposition system (PADs) developed by this team in this project.

ADVANTAGE BUSINESS 39242 12-9-14

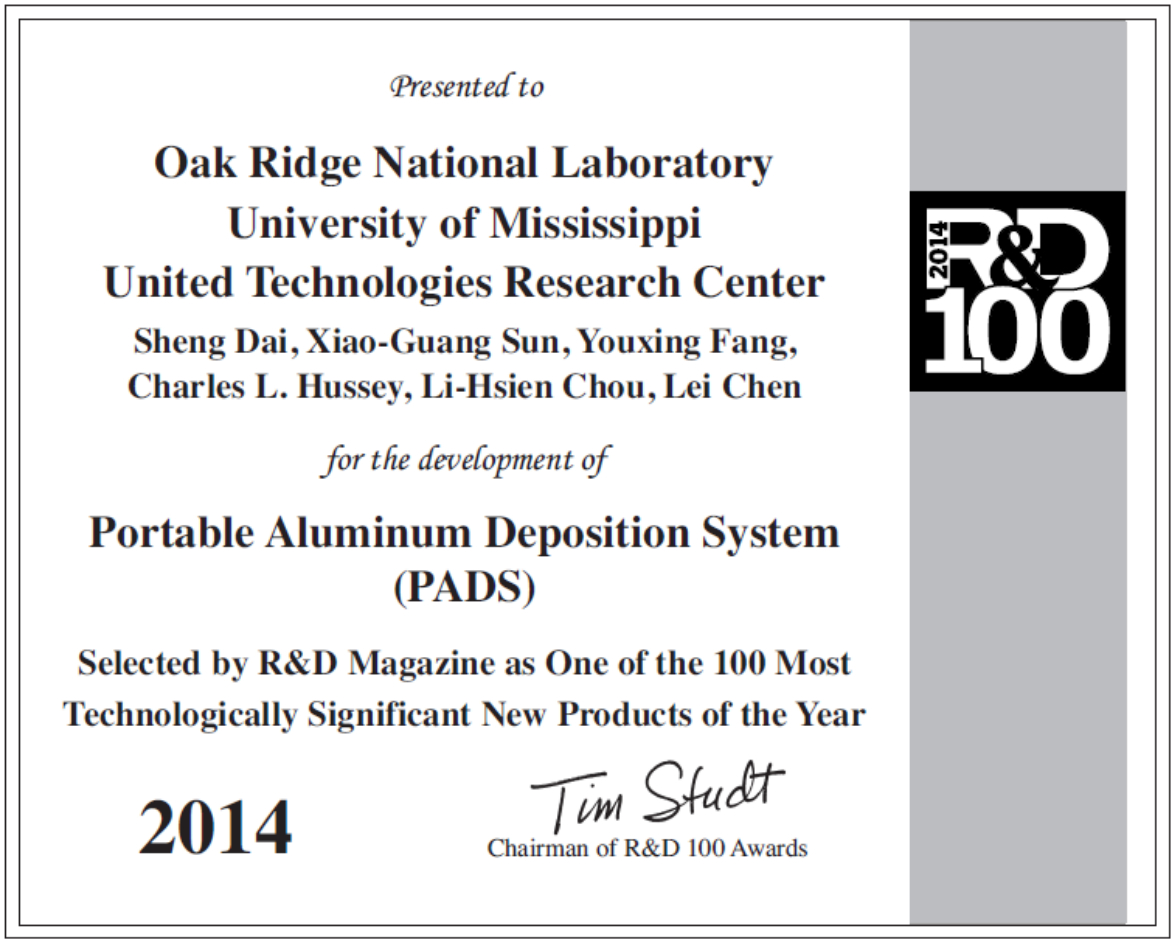

6 Addressing concerns of the technical committee

1. Please address what the unique military applications are for this electroplating process.

The ionic liquids electrolytes developed in this proposal can be used for aluminum deposition either in electrolyte bath or in portable aluminum plating system (PADs). In the former process the plating parts will be defined by the size of the electrolyte bath while in the latter process it can only be used for the surface plating, as it can't be used for internal diameters and complex geometries.

Both process can be used for military applications. Because of the non-flammability of the ionic liquids, it has less safety issues such as fire and flammability. Therefore, electroplating can be carried out in big electrolyte bath where the large pieces to be plated can fit in, provided moisture and oxygen are controlled so that they will not influence the plating process. This process can be carried out at the DoD depots facilities. On the other hand, PADs can be used for on-field repair for military applications. The repair can be easily carried out on-field under an inert gas blanket using either a portable potentiostat or simply battery pack. Depending on the size of the pieces to be plated, PADs can be scaled up accordingly. In this case, it eliminates transportation of the repair pieces to and from the depots, which can save money and time for the repair.

2. The technical committee expressed concerns with the toxicity and flammability of toluene and other solvents being used. Please address this issue in your Final Report.

We only used toluene in our experiments for comparison, it is not necessary to be used in practical applications. As to other organic functional starting materials used to prepare the ionic liquids, they do not exist as neutral molecules anymore, as they have been converted to the ionic liquids, which have high thermal stability (above 200 ^{o}C) and nonflammable so that they can be used for ambient temperature plating and higher temperatures below 100 ^{o}C without safety concerns.

3. In your Final Report, please address limitations to the coating thickness as well as applications to internal diameters and complex geometries.

As demonstrated in the report (page 38) that the aluminum coating thickness increases with plating time. Using 1.5 V battery, an aluminum coating thickness of 12 μm can be obtained in 30 minutes, which can be increased to 25 μm if the plating time is increased to 60 minutes. This result indicates that the coating thickness increases almost linearly with the plating time, that is, a coating thickness of 50 μm and 100 μm can be obtained in 2 and 4 hours, respectively. However, as the coating grows in thickness, it tends to become dendritic and movement of the deposition pen tends to dislodge the deposit and prevent further growth of the film thickness. On the other hand, it should be emphasized that the above plating is carried out inside the glovebox. If the plating is carried out using PADs outside the glovebox with an inert gas being connected, the plating should be carried out within the shortest time to minimize the interference of the moisture and oxygen from the air. For practical application, the benefit of gaining thickness versus

interference from air should be carefully considered. As mentioned previously, the PADs can't be used for plating on internal diameters and complex geometries.

References

1. Zhao, Y. and T.J. VanderNoot, *Electrodeposition of aluminum from nonaqueous organic electrolytic systems and room temperature molten salts.* Electrochimica Acta, 1997. **42**: p. 3-13.
2. Legrand, L., et al., *Sulfone-based electrolytes for aluminum electrodeposition.* Electrochimica Acta, 1995. **40**: p. 1711-16.
3. Omote, A., *Non-aqueous electrolyte and secondary battery containing same.* US patent, 2009. **US7524587B2**.
4. Hurley, F.H., *Electrodeposition of aluminum*. 1948, US Patent 2446331.
5. Wier Jr, T.P. and F.H. Hurley, *Electrodeposition of aluminum*. 1948, US Patent 2446349.
6. Wilkes, J.S., et al., *Dialkylimidazolium Chloroaluminate Melts - a New Class of Room-Temperature Ionic Liquids for Electrochemistry, Spectroscopy, and Synthesis.* Inorg. Chem., 1982. **21**(3): p. 1263-1264.
7. Li, B., et al., *Pulse current electrodeposition of Al from an AlCl3-EMIC ionic liquid* Electrochimica Acta 2011. **56**: p. 5478-5482.
8. Johnston, M., et al., *Electrochemistry in ultrahigh vacuum: underpotential deposition of Al on polycrystalline W and Au from room temperature AlCl(3)/1-ethyl-3-methylimidazolium chloride melts.* J Phys Chem B, 2005. **109**(22): p. 11296-300.
9. Chang, J.K., et al., *Electrodeposition of Al coating on Mg alloy from Al chloride/1-ethyl-3-methylimidazolium chloride ionic liquids with different Lewis acidity.* Transactions of the Institute of Metal Finishing, 2008. **86**(4): p. 227-233.
10. Tsuda, T., et al., *Electrochemistry of titanium and the electrodeposition of Al-Ti alloys in the Lewis acidic aluminum chloride-1-ethyl-3-methylimidazolium chloride melt.* J. of Electrochem. Soc., 2003. **150**(4): p. C234-C243.
11. Pitner, W.R., C.L. Hussey, and G.R. Stafford, *Electrodeposition of nickel-aluminum alloys from the aluminum chloride-1-methyl-3-ethylimidazolium chloride room temperature molten salt.* J. of Electrochem. Soc., 1996. **143**(1): p. 130-138.
12. Liao, Q., et al., *Electrodeposition of aluminum from the aluminum chloride-1-methyl-3-ethylimidazolium chloride room temperature molten salt plus benzene.* J. of Electrochem. Soc., 1997. **144**(3): p. 936-943.
13. Atwood, D.A., *Cationic group 13 complexes.* Coordin. Chem. Rev., 1998. **176**: p. 407-430.
14. Abood, H.M., et al., *Do all ionic liquids need organic cations? Characterisation of [AlCl2.nAmide]+ AlCl4(-) and comparison with imidazolium based systems.* Chem Commun (Camb), 2011. **47**(12): p. 3523-5.
15. Wibowo, R., S.E.W. Jones, and R.G. Compton, *Kinetic and Thermodynamic Parameters of the Li/Li+ Couple in the Room Temperature Ionic Liquid N-Butyl-N-methylpyrrolidinium Bis(trifluoromethylsulfonyl) Imide in the Temperature Range 298-318 K: A Theoretical and Experimental Study Using Pt and Ni Electrodes.* J. of Phys. Chem. B, 2009. **113**(36): p. 12293-12298.
16. Song, J.Y., Y.Y. Wang, and C.C. Wan, *Review of gel-type polymer electrolytes for lithium-ion batteries.* J. of Power Sources, 1999. **77**(2): p. 183-197.

17. Stephan, A.M., *Review on gel polymer electrolytes for lithium batteries.* Eur. Polym. J., 2006. **42**(1): p. 21-42.
18. Liao, C., X.G. Sun, and S. Dai, *Crosslinked gel polymer electrolytes based on polyethylene glycol methacrylate and ionic liquid for lithium ion battery applications.* Electrochimica Acta, 2013. **87**: p. 889-894.
19. Liao, Q., et al., *Electrodeposition of aluminum from the aluminum chloride-1-methyl-3-ethylimidazolium chloride room temperature molten salt plus benzene.* J. Electrochem. Soc., 1997. **144**(3): p. 936-943.
20. Wilkes, J.S., J.S. Frye, and G.F. Reynolds, *AL-27 AND C-13 NMR-STUDIES OF ALUMINUM-CHLORIDE DIALKYLIMIDAZOLIUM CHLORIDE MOLTEN.* Inorg. Chem., 1983. **22**(26): p. 3870-3872.
21. Abood, H.M., et al., *Do all ionic liquids need organic cations? Characterisation of [AlCl2.nAmide]+ AlCl4(-) and comparison with imidazolium based systems.* Chem. Commun. (Camb), 2011. **47**(12): p. 3523-3525.
22. Dalibart, M., J. Derouault, and P. Granger, *SPECTROSCOPIC INVESTIGATIONS OF COMPLEXES BETWEEN ACETONITRILE AND ALUMINUM TRICHLORIDE .2. STUDY OF ALCL3 IN ACETONITRILE MIXTURES OF TETRAMETHYLAMMONIUM CHLORIDE, WATER, OR NITROMETHANE.* Inorg. Chem. , 1982. **21**(6): p. 2241-2246.
23. Dalibart, M., et al., *SPECTROSCOPIC INVESTIGATIONS OF COMPLEXES BETWEEN ACETONITRILE AND ALUMINUM TRICHLORIDE .1. ALUMINUM-CHLORIDE ACETONITRILE SOLUTIONS.* Inorg. Chem. , 1982. **21**(3): p. 1040-1046.
24. Derouault, J. and M.T. Forel, *SPECTROSCOPIC INVESTIGATION OF ALUMINUM TRIHALIDE-TETRAHYDROFURAN COMPLEXES .1. STRUCTURE AND FORCE-FIELDS OF 1-1 AND 1-2 SOLID COMPOUNDS FORMED BY ALUMINUM-CHLORIDE OR BROMIDE.* Inorg. Chem. , 1977. **16**(12): p. 3207-3213.
25. Derouault, J., P. Granger, and M.T. Forel, *SPECTROSCOPIC INVESTIGATION OF ALUMINUM TRIHALIDE-TETRAHYDROFURAN COMPLEXES .2. SOLUTIONS OF ALUMINUM-CHLORIDE OR BROMIDE IN TETRAHYDROFURAN AND IN TETRAHYDROFURAN-DICHLOROMETHANE.* Inorg. Chem. , 1977. **16**(12): p. 3214-3218.
26. Sundaraganesan, N., N. Puviarasan, and S. Mohan, *Vibrational spectra, assignments and normal coordinate calculation of acrylamide.* Talanta, 2001. **54**(2): p. 233-241.
27. Fang, Y.X., et al., *An AlCl3 based ionic liquid with a neutral substituted pyridine ligand for electrochemical deposition of aluminum.* Electrochimica Acta, 2015. **160**: p. 82-88.
28. Fang, Y.X., et al., *New ionic liquids based on complexation of dipropylsulfide and AlCl3 for electrodeposition of aluminum.* Chem. Comm., 2015. **51**: p. 13286 – 13289.
29. https://en.wikipedia.org/wiki/Anodizing.
30. https://simple.wikipedia.org/wiki/Carbon_steel.